November 2004 • NREL/SR-520-36983

Subcontractor Report

Trajectory Oriented and Fault Tolerant Based Intelligent Process Control for Flexible CIGS PV Module Manufacturing Scale-Up

Phase II, Annual Technical Report March 2004

L. Simpson
ITN Energy Systems, Inc.
Littleton, Colorado

National Renewable Energy Laboratory
1617 Cole Boulevard, Golden, Colorado 80401-3393
303-275-3000 • www.nrel.gov

Operated for the U.S. Department of Energy
Office of Energy Efficiency and Renewable Energy
by Midwest Research Institute • Battelle

Contract No. DE-AC36-99-GO10337

November 2004 • NREL/SR-520-36983

Trajectory Oriented and Fault Tolerant Based Intelligent Process Control for Flexible CIGS PV Module Manufacturing Scale-Up

Phase II, Annual Technical Report March 2004

L. Simpson
ITN Energy Systems, Inc.
Littleton, Colorado

NREL Technical Monitor: R. Mitchell

Prepared under Subcontract No. ZDO-2-30628-07

National Renewable Energy Laboratory
1617 Cole Boulevard, Golden, Colorado 80401-3393
303-275-3000 • www.nrel.gov

Operated for the U.S. Department of Energy
Office of Energy Efficiency and Renewable Energy
by Midwest Research Institute • Battelle

Contract No. DE-AC36-99-GO10337

Executive Summary

ITN Energy Systems, Inc., and Global Solar Energy, Inc., with the assistance of NREL's PV Manufacturing R&D program have continued the advancement of CIGS production technology through the development of trajectory oriented predictive/control models, fault tolerance control, control platform development, in-situ sensors, and process improvements. Modeling activities to date include the development of physics-based and empirical models for CIGS and sputter deposition processing, implementation of model-based control, and application of predictive models to the construction of new evaporation sources and for control. Model-based control is enabled through implementation of reduced or empirical models into a control platform. Reliability improvement activities include implementation of preventive maintenance schedules; detection of failed sensors/equipment and reconfiguration to continue processing; and systematic development of fault prevention and reconfiguration strategies for the full range of CIGS PV production deposition processes. In-situ sensor development activities have resulted in improved control and indicated the potential for enhanced process status monitoring and control of the deposition processes. Substantial process improvements have been made, including significant improvement in CIGS uniformity, thickness control, efficiency, yield, and throughput. In large measure, these gains have been driven by process optimization, which in turn have been enabled by control and reliability improvements due to this PV Manufacturing R&D program. This has resulted in substantial improvements of flexible CIGS PV module performance and efficiency.

Table of Contents

List of Figures

1. Background

Interest in thin film photovoltaics (PV) has expanded dramatically, but wide-scale commercial use remains limited by performance and cost. These factors are often interrelated and negatively impacted by the lack of reliable and accurate process control. ITN Energy Systems, Inc. (ITN) and Global Solar Energy, Inc. (GSE) are using a comprehensive and systematic program to integrate intelligent process control into the manufacture of flexible, lightweight copper indium gallium diselenide (CIGS) based PV modules. Process control has been a priority since the outset of this endeavor, enabling the development of a fully integrated CIGS module manufacturing facility in only four years. GSE's production facility is fully equipped for manufacturing flexible, lightweight CIGS PV products. Key CIGS manufacturing facilities includes: molybdenum back contact, large-area CIGS absorber layer, cadmium sulfide, and transparent conductive oxide deposition systems; fully automated laser scribing; module lamination, and PV product finishing equipment. Each production deposition system is capable of processing 12-in. wide 1000-ft. long polymer or stainless steel in a low cost, automated fashion. The PV Manufacturing R&D program aims to enable GSE/ITN to complete a fully integrated process control development program with models, control platform, and diagnostic tools (sensors) for intelligent processing of PV modules, with the ultimate goal of improving CIGS module performance, process throughput, and yield.

To capitalize on the potential cost reductions that thin film processing methods can provide for polycrystalline PV modules, every manufacturing step must be controlled at a level where quality and yield are maximized. Depending on the complexity and extent of fundamental scientific understanding of each process, the transition to large-scale manufacturing can be more difficult and costly than anticipated. A critical requirement is the development and implementation of diagnostic tools and associated predictive models that can quantitatively assess the relationship of processing conditions to product properties.

In general, diagnostic capabilities for manufacturing thin films are rudimentary, and manufacturers can only assess their product after module completion. Inadequate diagnostics and predictive models result in sub-optimal control and correspondingly lower quality and yield. For system failures, the most common strategy consists of sophisticated interlocking and alarm mechanisms to stop the process when a fault is detected. Process models/simulators are required for unanticipated process upsets, reactor variability/drift, and operation in unstable processing regimes where repeatability can be achieved only through dynamic feedback/feed-forward control. Similarly, in-situ, real-time process diagnostics development, in the form of sensors, is also required since their use has been proven to improve process yield/quality and reduce module costs.

The essence of our PV Manufacturing R&D effort is to develop trajectory oriented and fault tolerance based intelligent process control using predictive physics-based process models and strategic process/film property sensors to significantly improve yield, throughput, and performance of flexible CIGS PV modules. Implementation of trajectory-oriented control consists of four tasks, specifically, development of mathematical relationships (models) between control variables and final product properties (system identification), reduction of models into computationally efficient form(s), establishment of optimum trajectories for film properties during deposition and implementation into a control platform. Fault tolerance activities include detection, location, and isolation of faults, and implementation of appropriate corrective actions that minimize faults from becoming critical failures. Diagnostic tool activities involve integration of existing and alternative sensors to increase reliability and/or provide process information. All effective model/sensor features are incorporated into a robust control platform that will enable autonomous and continuous manufacturing, with automatic data storage and presentation for operator monitoring.

1.1. Review of Phase I Activity

During Phase I, ITN Energy Systems, Inc. research efforts included:

- The development of trajectory-oriented models for control of Mo and CIGS production deposition systems;

- The detection and location of potential faults in production Mo and CIGS deposition systems;
- The development of software that enabled hardware interfacing, model implementation and graphical user interfaces; and
- The investigation of the feasibility and utility of implementing new and/or existing diagnostic tools in the Mo, CIGS, CdS, and ITO deposition systems on CIGS production systems.

Model Development - In the first year, several models were developed and integrated for CIGS production systems. These included:

- *Finite Element (FE) Thermal* – A physics-based finite element thermal model of the effusion cells, with 2606 nodes, was developed in ABAQUS.[i]
- *Melt Convection* – A reservoir flow model was developed with the heat transfer model to determine the vapor flow in the source above the melt and to determine the conditions at the source outlets. From this vapor flow model, the conditions at specific points within the source can be determined (pressure, velocity, and mass flow rates).
- *Boundary-layer Flow* – The vapor flow model results are then put into a source outlet boundary-layer flow model, based on one of the codes in the CHEMKIN suite.[ii] This model is used to determine the nucleation behavior of droplets forming in the source outlet.
- *Plume Interaction* – The vapor flow results are also used as inputs to a Direct Simulation Monte Carlo (DSMC)[iii] module of the effusion source plumes. This enables investigation of plume interaction effects (including back-pressure at the source), and provides predictive plume shape capabilities to improve thin film thickness uniformity across the substrate.
- *Deposition* – Initial modeling efforts of the heat transfer to the web include effusion source surroundings, reactor geometries, and web/heater assembly configurations. This model was created and analyzed using ABAQUS; results from the effusion source models were simplified and applied as boundary conditions. Model results will provide insight to web heating changes with source outlet geometry changes, as well as an effective heater model to predict thermal gradients throughout the web.[iv]

In addition to model development for evaporation and sputtering, initial model validation and reduction was performed. This involved tuning parameters to a particular reactor by perturbing process inputs and recording the response with available process sensors. A related process occurs for model reduction, where the reduced model structure is a generic low order differential equation or response surface, rather than specific physical laws. These models can then be used to determine input trajectories and to determine internal states given sensor measurements. In addition, the source models provided temperature relationships between the melt and source outlet, predicted outlet dynamics including condensation, and predicted system time constants for transient input conditions. Therefore, the source models were used to predict quantifiable differences in source design changes to identify/validate improvements. Initial source design improvements resulted in significantly enhanced side-to-side uniformity and considerable reduction in the potential for recondensation in the effusion source outlet. Source redesign efforts have eliminated several undesirable operating characteristics and have substantially improved stability of the flux delivery, thus minimizing thickness variation, as shown in Figure 1.

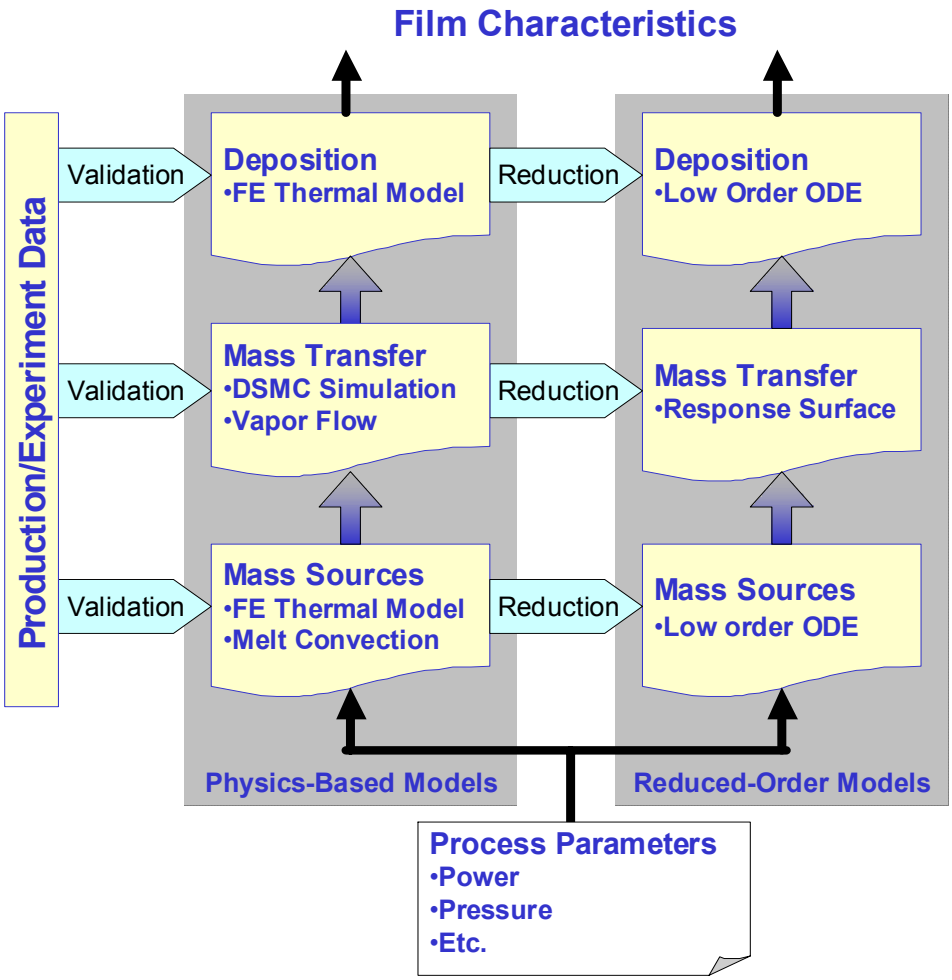

Figure 1. Outline of the individual modules combined to provide an overall model of CIGS processing

Model-Based Process Control **–** In addition to providing predictive information about each component in the process, models were utilized to provide improved control of individual element deposition from each CIGS source. Model-based control has been implemented for all the deposition sources (NaF, In, Ga, Cu, and Se) based on sensor input and non-linear dynamic models. Compared to simple PID control, model-based control is advantageous for decreased thickness variation of individual constituents, as shown in Figure 2, corresponding to better control of film properties including Cu/(In+Ga) and Ga/(In+Ga) ratios. Process modifications resulting from model-based control combined with improved source design have begun to show improvements in overall yield. Additional gains in average efficiency and yield were expected with parameter optimization and further refinements in process control.

Reliability - The reliability of production systems was improved by fault prevention and fault tolerance. Thus, initial diagnostic evaluations of reconfiguration strategies for all levels of the CIGS PV production deposition systems were performed. In addition, specific subsystems were identified where implementation of fault tolerance methodologies could be beneficial. The initial fault tolerance issues identified included:

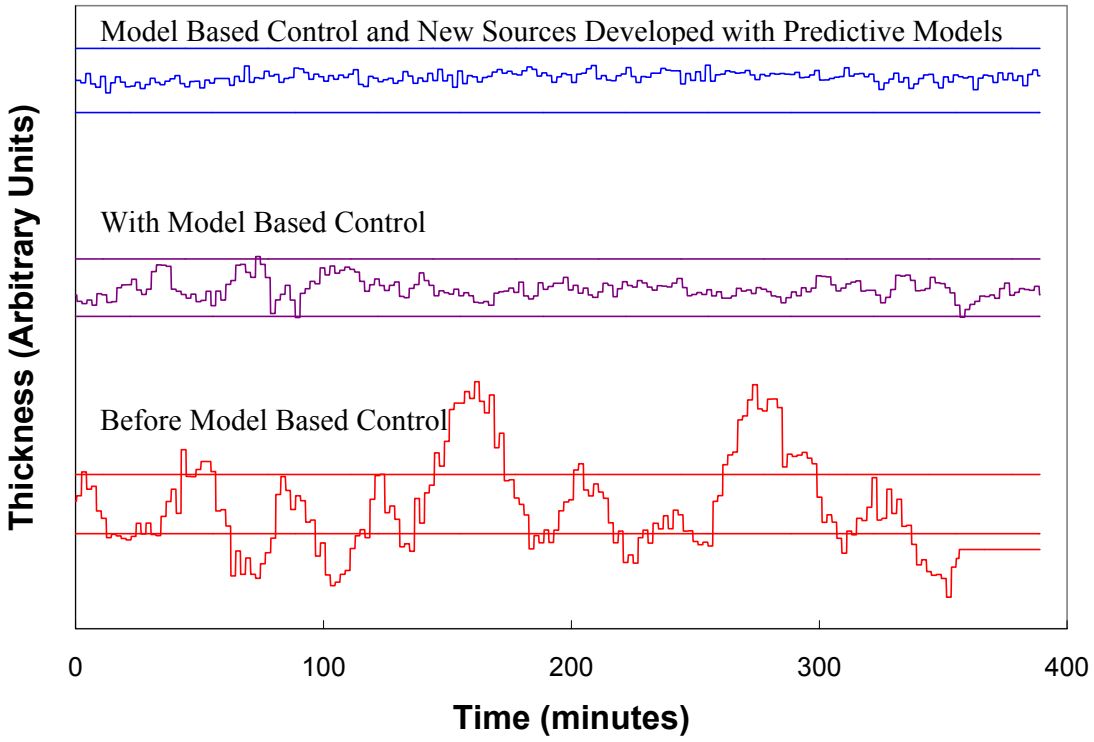

Figure 2. Comparison of thickness variability improvements with improved model developments; the solid lines indicate +/- 5% from the average

- Source thermocouple accuracy and failures
- Sodium fluoride sensor reliability
- Substrate heater failures
- Line voltage regulation
- Source power and current, and
- Sputtering source arc detection.

To enhance system reliability further, a systematic evaluation of equipment failures was performed and a preventive maintenance schedule developed. In addition, redundant operator input was implemented to decrease the relatively high incidence of system faults induced by input error. The main reconfiguration strategies incorporated included redundant components and alternative sensor control.

Sensors - As part of the initial PV Manufacturing R&D effort, several specific control parameters of all the PV production deposition systems were identified where benefits could be realized with in-situ diagnostics. Once specific concepts were identified, importance and feasibility criteria were applied to narrow the scope of effort to provide maximum results with the given resources. After considering all of the different factors, several sensor development activities were initiated for Phase I, including:

- Investigation of RGA, OES, and QCMs to provide flux and chamber health monitoring for the Mo and ITO sputtering systems
- Development of pyrometry to improve source and substrate temperature monitoring
- Investigation of emissometry to measure film temperature, roughness, and emissivity
- Development of Se flux monitoring

- Development of alternative input current/voltage measurement methodologies to monitor system health and provide process control
- Investigation of reflectometry to provide characteristics of the various coatings, and
- The use of visible imaging for CdS film thickness.

Year 1 Summary - In the first year of the PV Manufacturing R&D program, steady improvements in processing and increased yields of large area cells occurred with efficiencies typically ranging between 4 and 8% (Figure 3). Initial efforts to improve process control and fault tolerance along with preventive maintenance schedules lowered fault events and provided well-controlled deposition of individual CIGS elements (Figure 2). Models were used to provide both revolutionary new evaporation source and substantial process control improvements. In addition, initial fault prevention and tolerance activities have increased reliability and identified several areas where reconfiguration/recovery methodologies can be applied. Finally, initial development activities have identified several sensors that could or have improved process control

1.2. Overview of Phase 2 Activity

During Phase II, research efforts included:

- The design and implementation of trajectory oriented control models on production deposition systems;
- Development of control models/algorithms for sputter deposition systems;
- Evaluation of the performance of the fault tolerance strategy; and
- Implementation of reduced models, control algorithms, and new sensors into production systems.

These activities in Phase II have resulted in outstanding improvements in CIGS cell performance, even greater than that obtained with the Phase I effort. Figure 3 illustrates the improvement from Phase 1 to Phase 2. In general, since the inception of this program, average and maximum efficiencies have increased substantially (Figure 4). Since this program is primarily directed at increasing average efficiency, the fact that average efficiency (normalized) has increased by more than a factor of two compared to the maximum efficiency is an indication of the benefits obtained from this PV Manufacturing R&D program. The main benefits from the different activities of the program have resulted from substantially improved control/yields providing improved systematic evaluation through "design of experiments" that enable process parameters that lead to improved performance to be more quickly identified and reproducibly obtained in production.

Cell yields have also improved during the project (Figure 5 and Figure 6). An increase of greater than four fold has occurred since the inception of this program and a significant amount of that increase can also be directly attributed to PV Manufacturing R&D activities. Continued efforts to improve fault tolerance through model-based diagnosis and decision-making algorithms have lowered fault events (Figure 7) and provided well-controlled deposition of individual CIGS elements (Figure 8). Thus, in general, the expectations for CIGS PV performance improvements at the outset of the PV Manufacturing R&D program have been far exceeded with the potential for improvement still high due to the remarkable accomplishments that have been made for the CIGS processes. The Phase III efforts will build upon these tremendous accomplishments to complete several process control and fault tolerance tasks and implement additional improvements in processing.

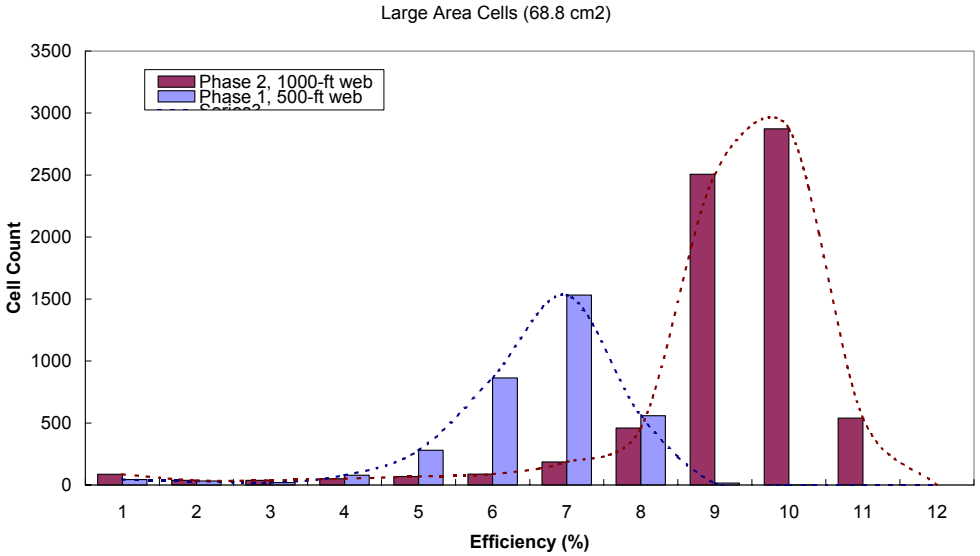

Figure 3. Comparison of cell efficiency and count for individual runs in Phase 1 and Phase 2

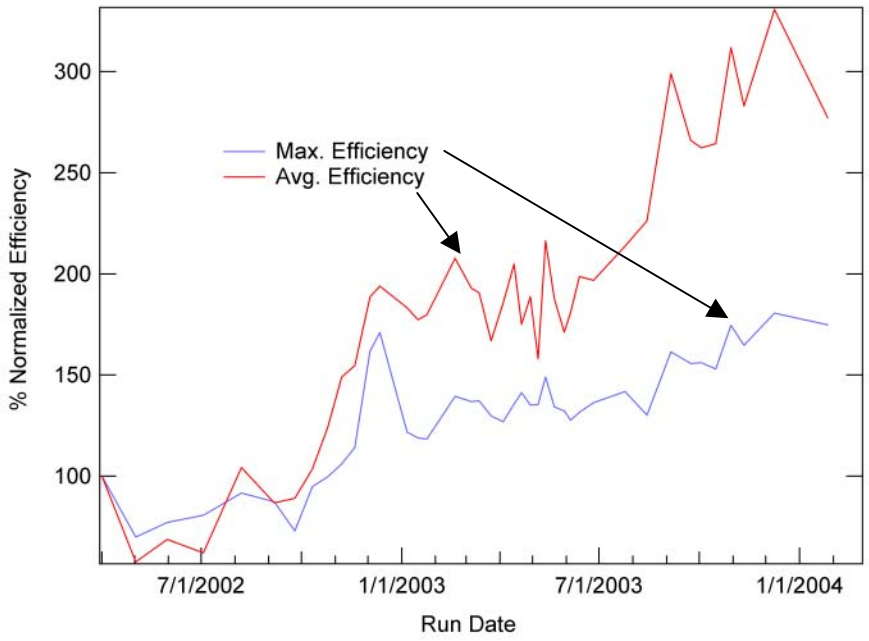

Figure 4. Normalized increase in efficiencies of production PV since inception of PV Manufacturing R&D Program

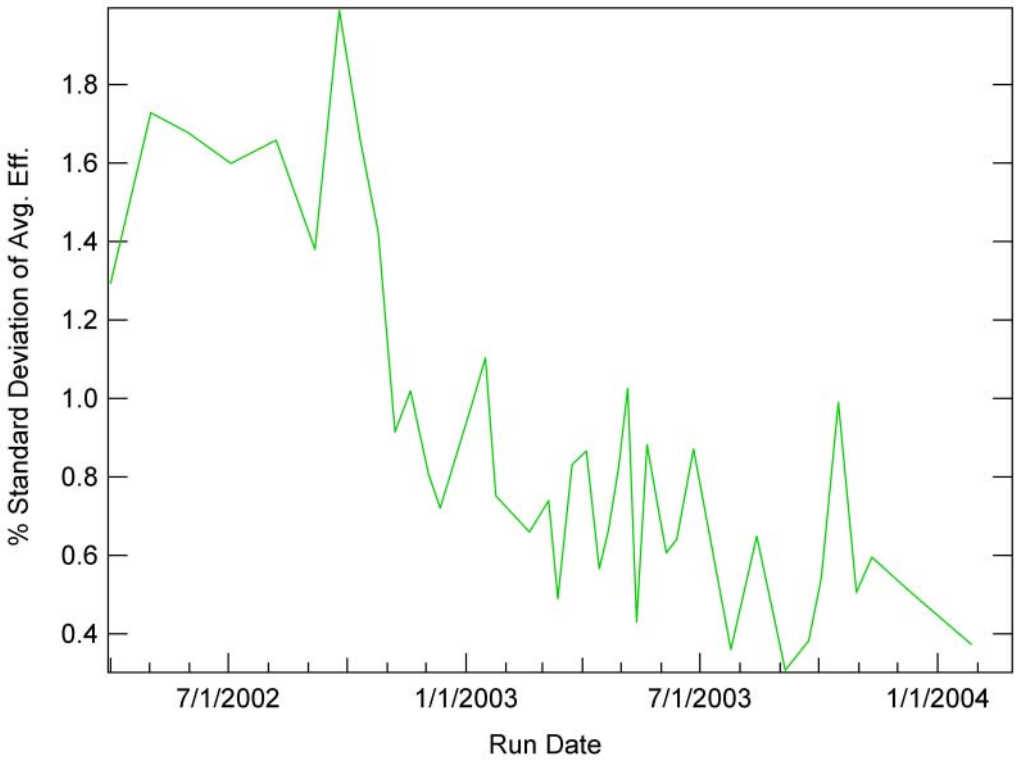

Figure 5. Standard deviation of average efficiencies (in absolute %) over time has decreased

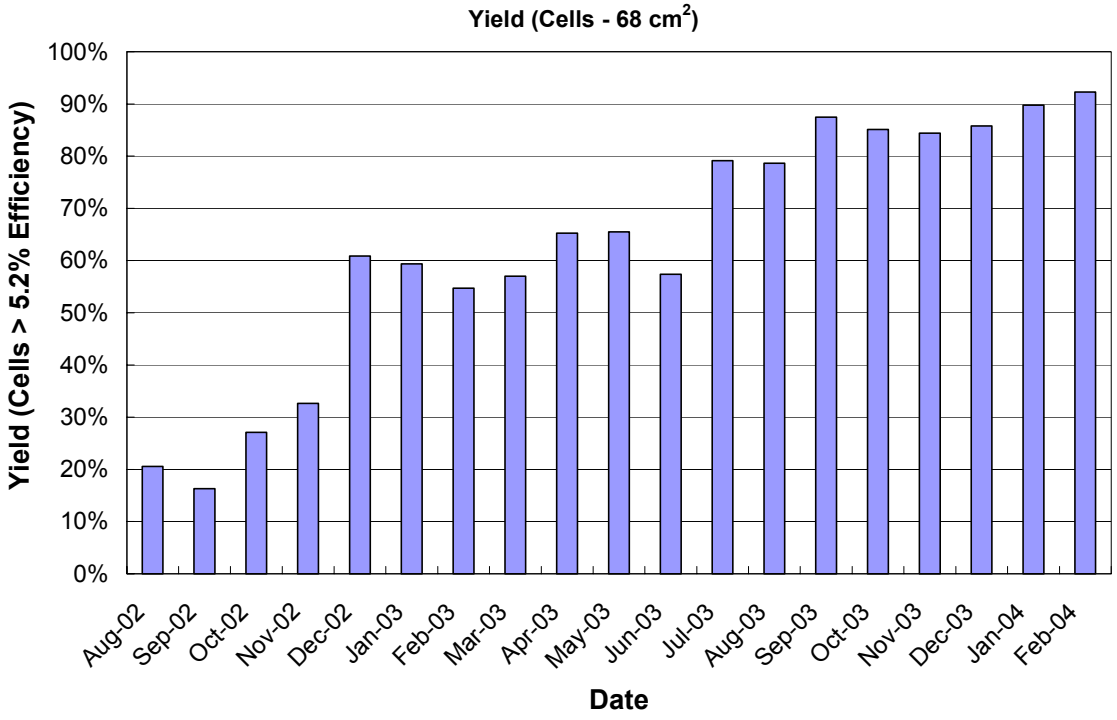

Figure 6. Time line of cells yielded from CIGS production

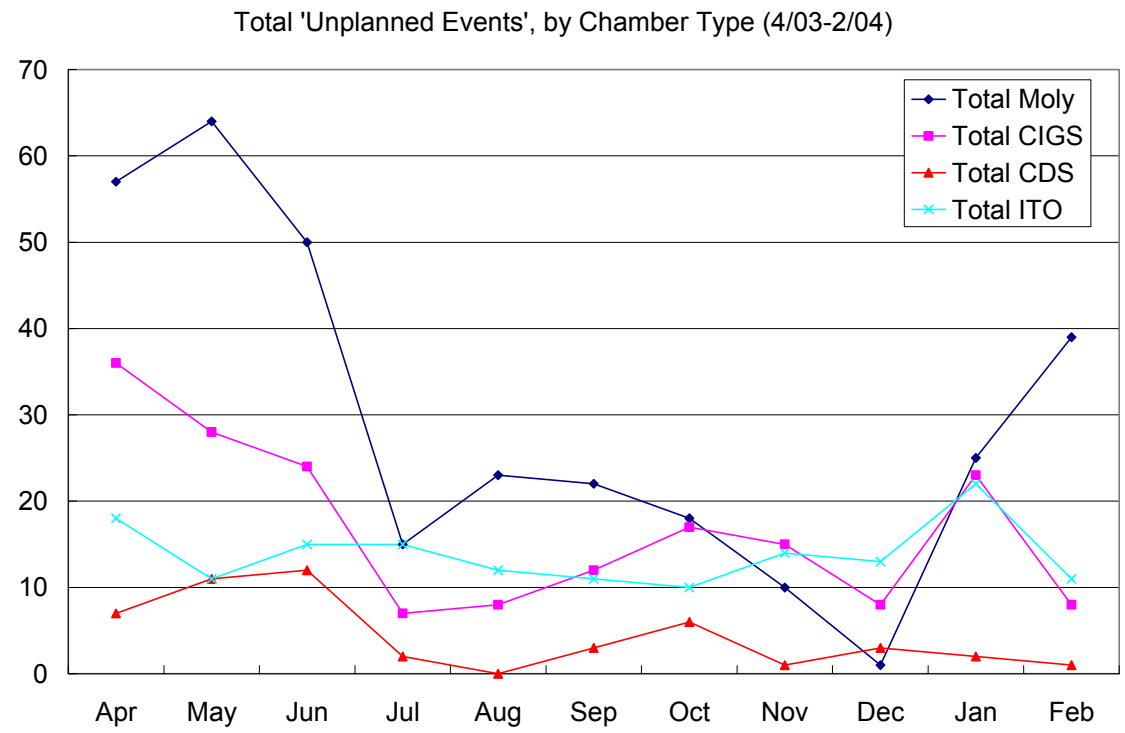

Figure 7. Frequency of anomalies or unplanned deviations (incidents) per 1000 ft. for different deposition processes

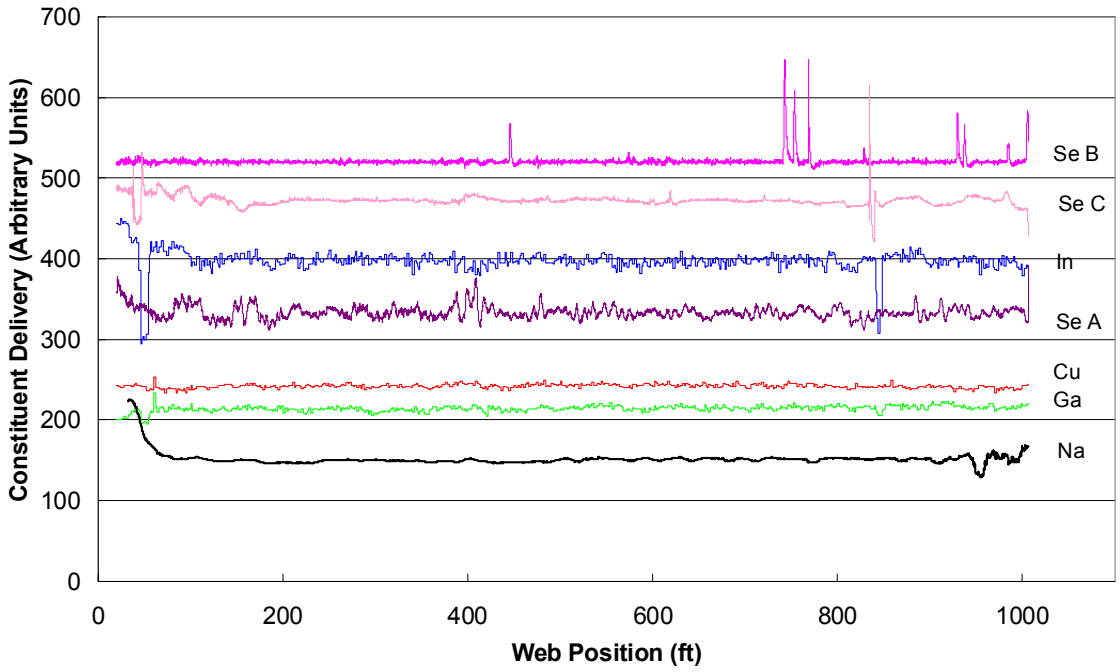

Figure 8. Real-time composition and flux signals monitored by in-situ sensors during a 1000 ft. CIGS deposition on stainless steel with active process control

2. Model Development

Model development has been an important area of focus during the second year of the PV Manufacturing R&D program. As discussed above, the models are used to improve the processes and hardware (e.g. evaporation sources), provide more robust dynamic control, and enable fault detection and recovery. The following sections describe the role of models for CIGS PV deposition systems.

2.1. Physics-Based Model Development

2.1.1. CIGS

Physics-based models are key for better understanding of the process and as an important component for improved process control. Information learned on droplet nucleation and plume uniformity has directly led to design changes of the thermal evaporation sources. Furthermore, models identify fast transient dynamics for feedback control as well as slower dynamic effects that require gradual set point adjustments.

The models developed have been focused in three areas – mass sources, mass transfer, and deposition (Figure 1). Production data is used for validation; however, the physics-based models are too complex to be used directly for process control. For this purpose, the physics-based models are simplified into reduced-order models, which are also validated by production data and operate approximately 2000 times faster than the full physics-based models.

Mass Source Model - Finite Element (FE) Thermal

A physics-based finite element thermal model of the effusion cells, with 2606 nodes, was developed in ABAQUS (Figure 9). The FE thermal model was originally developed to address poor cross web uniformity and nucleation/growth of particulates ("spitting") that were deposited on the substrate (Figure 10).

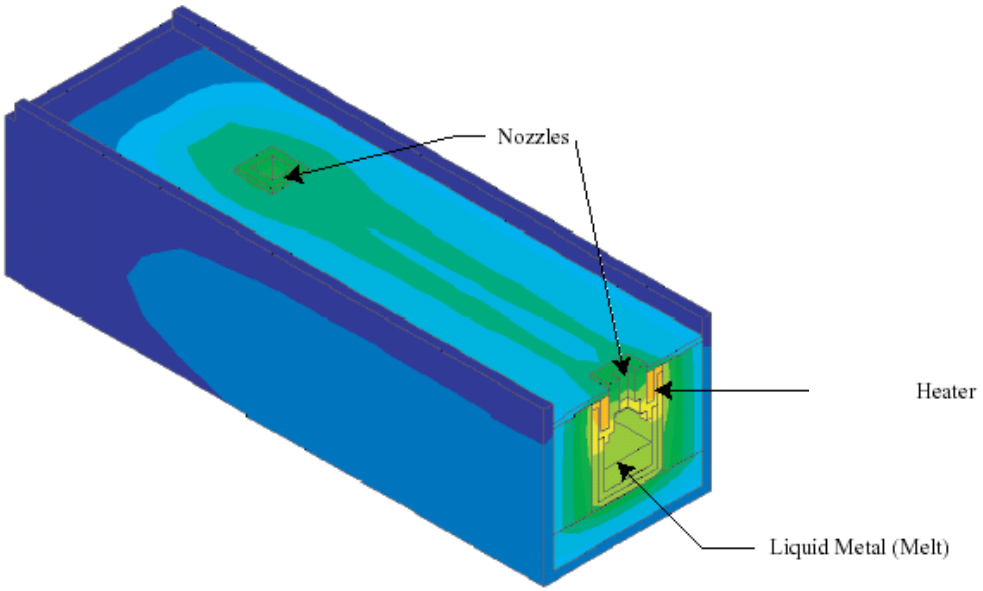

Figure 9. Finite Element ABAQUS Thermal Model of a thermal evaporation source

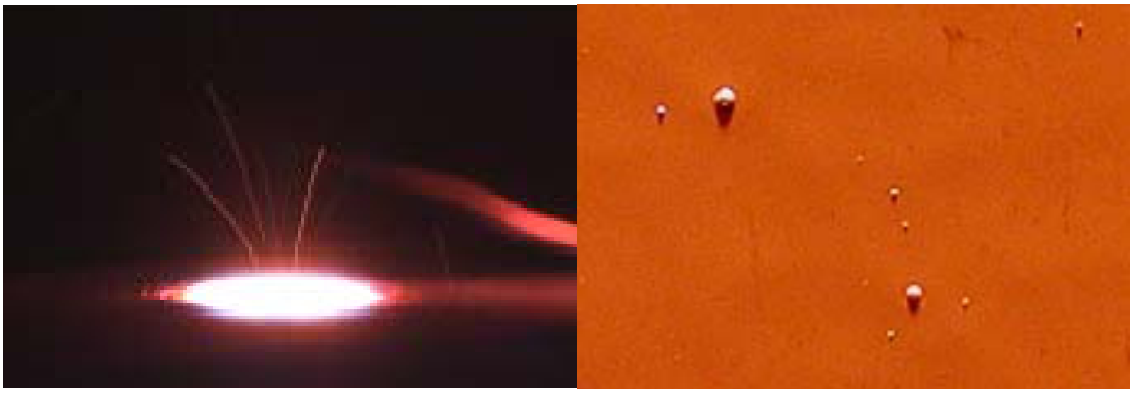

Figure 10. "Spitting" from the source nozzle (Left) causes particulates to form on the substrate (right). Courtesy of The Institute for Energy Conversion.

In year 1, a new source was designed based on information from this model. Year 2 efforts have increased the accuracy and adaptability of the ABAQUS model, improving the transient response predictability of the model. Figure 11 depicts thermocouple test data and the ABAQUS results for the equivalent power settings at various important locations. Note the solid line is ABAQUS data and the dashed is experimental.

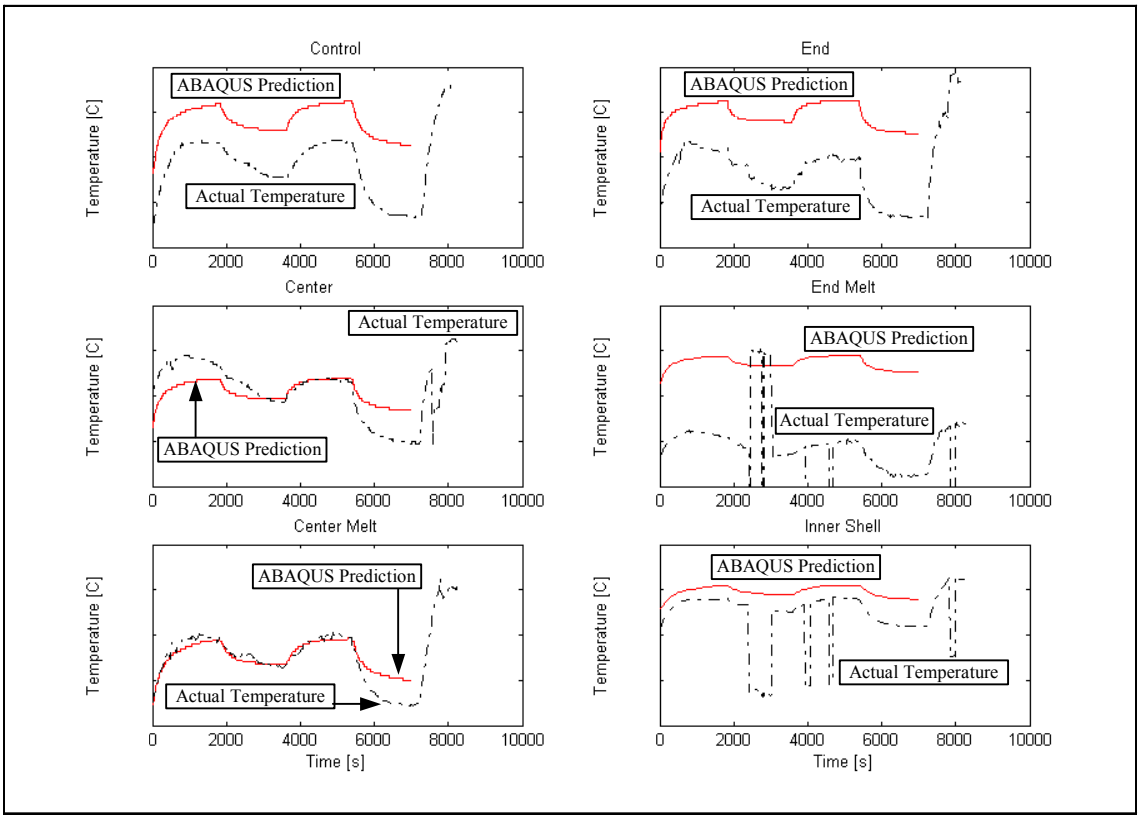

Figure 11. Comparison of Actual and ABAQUS Predictions of Source Temperature Responses. Note that the actual temperature responses have "drop outs" related to signal error, not actual changes.

To be useful for real-time process control, the validated FE thermal models are expressed using ordinary differential equations. Extension of previous source and chamber modeling work was done to produce more accurate reduced models that could be implemented for real-time processing. The reduction process was used to find the state space models of the system. For example, the ABAQUS effusion model was configured in nine different ways since there are three different metals and three different melt heights (10%, 50%, and 90%) to represent different periods during the deposition process. Reduced state models were determined for each combination and they compare well with the ABAQUS models. Figure 12 shows the system response of both a reduced model and the ABAQUS model for a 50% full copper source to a series of step inputs.

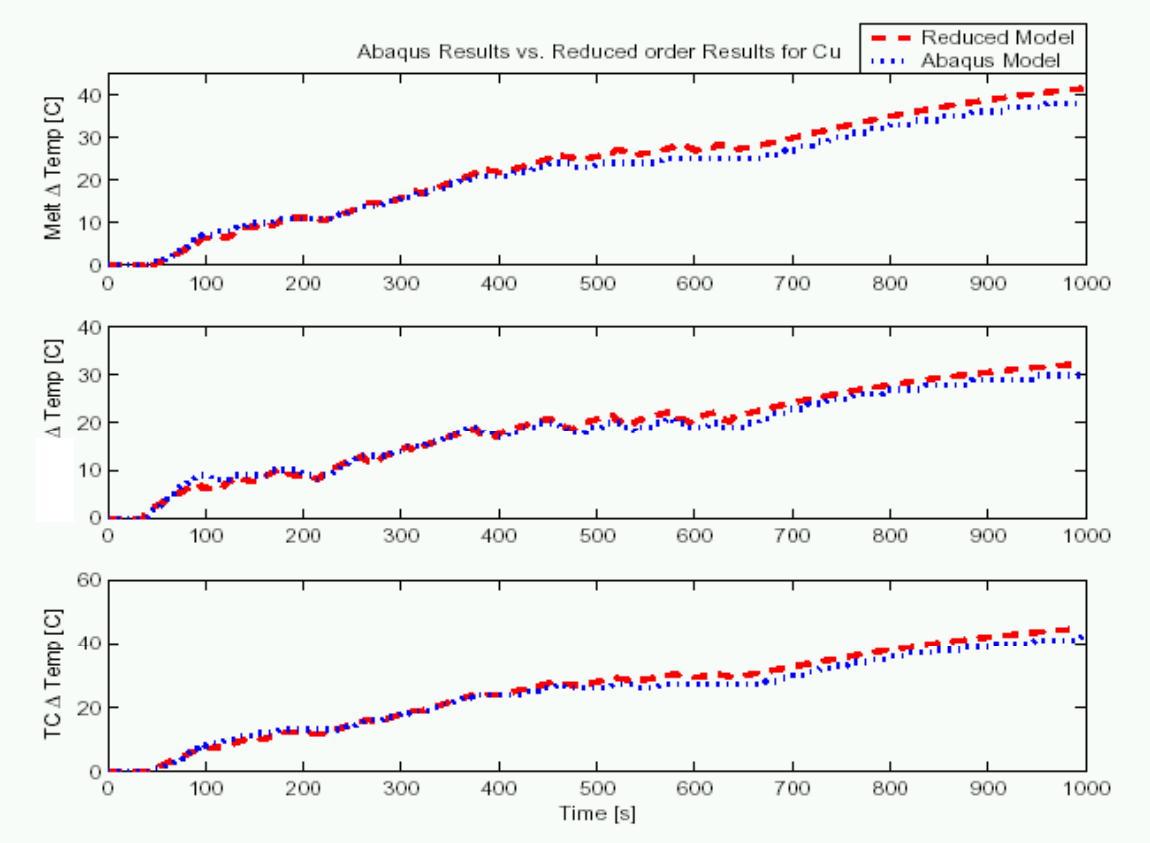

Figure 12. Comparison of ABAQUS and Reduced Models for different locations of a 50% Filled Cu Source

Multiple Effusion Source Rate Estimate

Presently, contributions from multiple effusion sources are determined from a process that renders the deposited film useless for PV. Thus, this procedure is used minimally and real-time contributions are unknown. Because of the nonlinear dependence of effusion rate on temperature, there is the possibility of obtaining information about the absolute effusion rate using only the change of effusion rate with temperature. If implemented, the procedure could increase yield by not taking the compositions out of bounds and could improve down-web uniformity to enhance efficiency. To evaluate how the contribution estimation will work, a simulation was performed using MATLAB. Based on these simulations, perturbations were designed and used to determine the contributions from multiple effusion sources.

The MATLAB simulation was developed along with several corresponding reduced gallium and indium models. These reduced models were incorporated into a simulation system with existing gallium and indium temperature controllers and set point estimators. A schematic of the methodology for developing reduced models is shown in Figure 13.

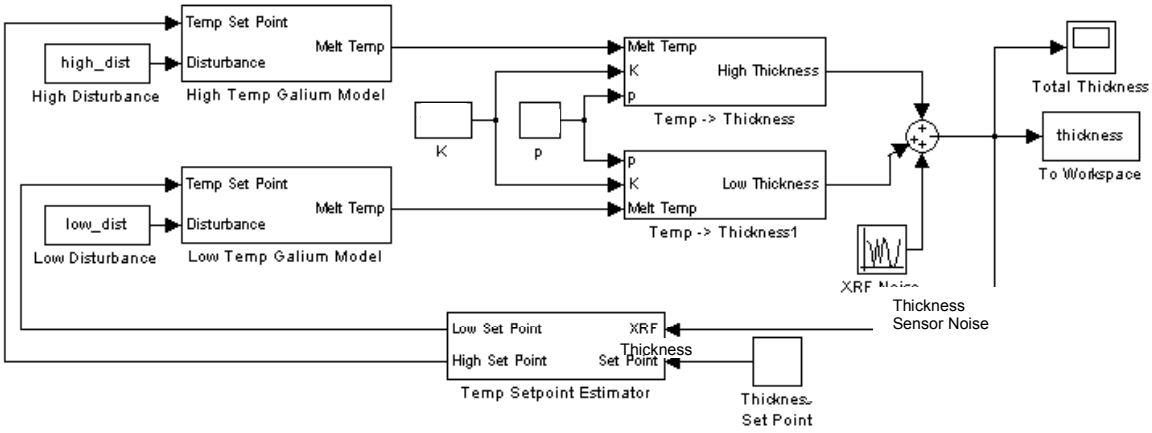

Figure 13. Schematic of MATLAB simulation for gallium rate estimation.

Running this simulation required an estimate of effusion rate from melt temperature. This is stated functionally as:

$$R_{Effusion} = Ke^{pT}$$

The goal of the simulations was to estimate ***K*** and ***p*** from measured thickness data, so ***K*** and ***p*** were selected and compared with the simulation estimates. Model outputs for both gallium and indium are shown in Figure 14 and Figure 15 and compared with the experimentally obtained system response from the CIGS deposition chamber where the perturbations were applied. The data in the figures demonstrate the ability of the models to provide accurate dynamic response predications, thus enabling unique measurement capabilities to determine the effusion rate from each source in a multiple source configuration. The goal is to be able to apply a short series of small temperature perturbations to the effusion sources to accurately calculate the contribution from each in a multiple source system. In addition, the models also provide predictions of the anticipated accuracies of the measurements based on the number and size of the perturbations and the noise in the deposition systems (Figure 15).

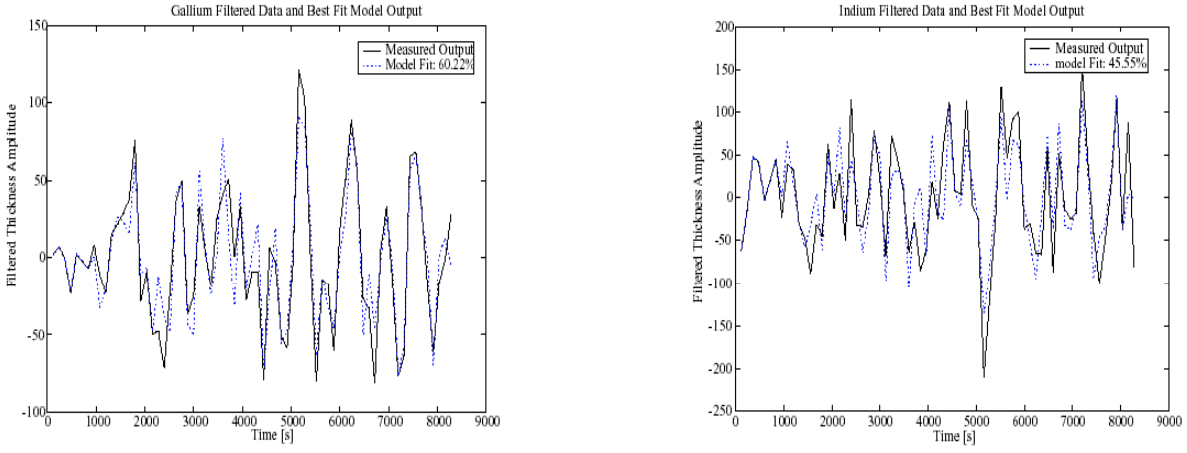

Figure 14. Filtered Gallium (left) and Indium (right) Data and Model Output

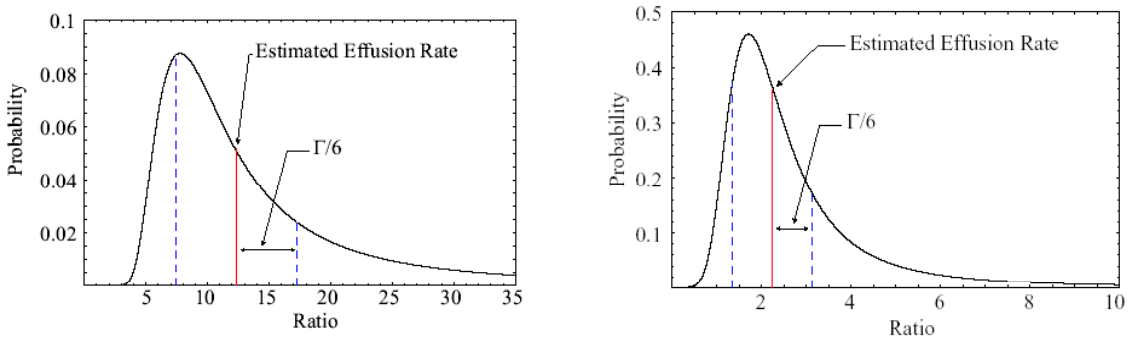

Figure 15. Ratio Probability Distribution for Gallium (left) and Indium (right) experiments indicate that the accuracy of the measurement will probably need to be improved to provide information for enhanced process control.

Mass Transfer Model – Direct Simulation Monte Carlo

The Direct Simulation Monte Carlo (DSMC)[iii] model enables investigation of plume interaction effects (including backpressure at the source), and provides predictive plume shape capabilities to improve thin film thickness uniformity across the substrate. Results of the DSMC model simulated vertical velocity field, temperature, ratio of critical diameter to hard sphere diameter, nucleation rate, and collision frequency. Representative plots of nucleation and growth rate are shown in Figure 16 with the cross section of the source outlet at the lower left corner. From these contour plots, it is evident that the gas rapidly expands to the near vacuum region at which the vapor flow accelerates and drops significantly in temperature. Regions of interest are the inner effusion source region and the bubble above the effusion source of colder temperature.

From the plot of nucleation rate (Figure 16), it is apparent that the bubble above the effusion source exit is the area of maximum nucleation due to the cold temperatures in this region. This area is even more important in that the ratio of critical diameter to hard sphere atom diameter is less than one. This means that nucleation in this region is collision controlled.[v]

Modeling has shown regions where the nucleation rate is very high, but the kinetic-theory collision frequency is quite small. Since the flow is moving at sonic (or greater) velocities in the source exterior where the nucleation rate is high, the residence time is very small. For substantial droplets to grow, there must be sufficient time for atom-atom collisions, and subsequently, time for a metal cluster to grow. Additional research is being conducted to create a model that will explain the process of droplet nucleation, including number of droplets and cluster size. Ultimately, understanding of droplet formation may enable source designs that eliminate this type of event, thus increasing yield and efficiency since droplets usually result in shorts.

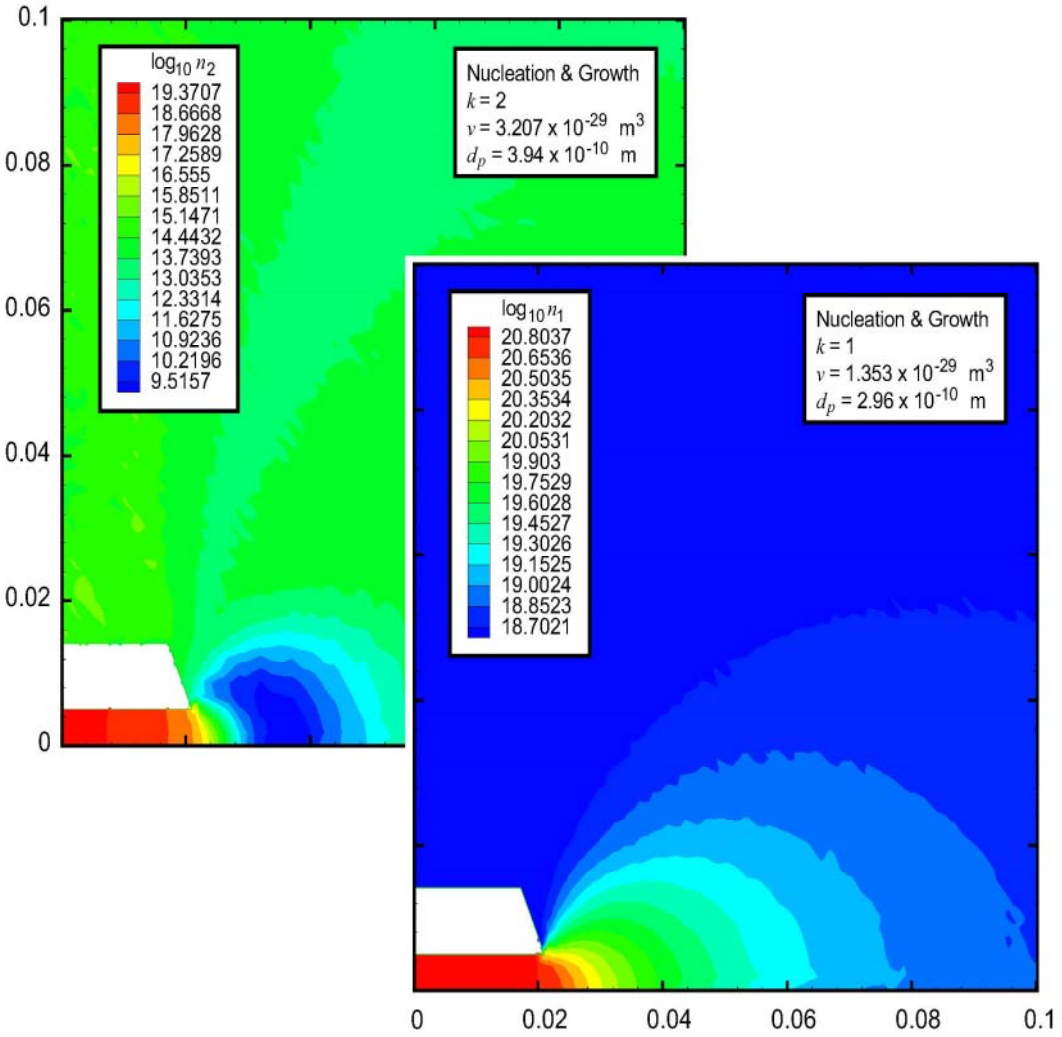

Figure 16. Contours of the size distribution function considering nucleation and growth by evaporation or condensation.

The plume model (Figure 17) is used in addition to the DSMC model and considers the effect of Se scattering in predicting plume shape and deposition uniformity.

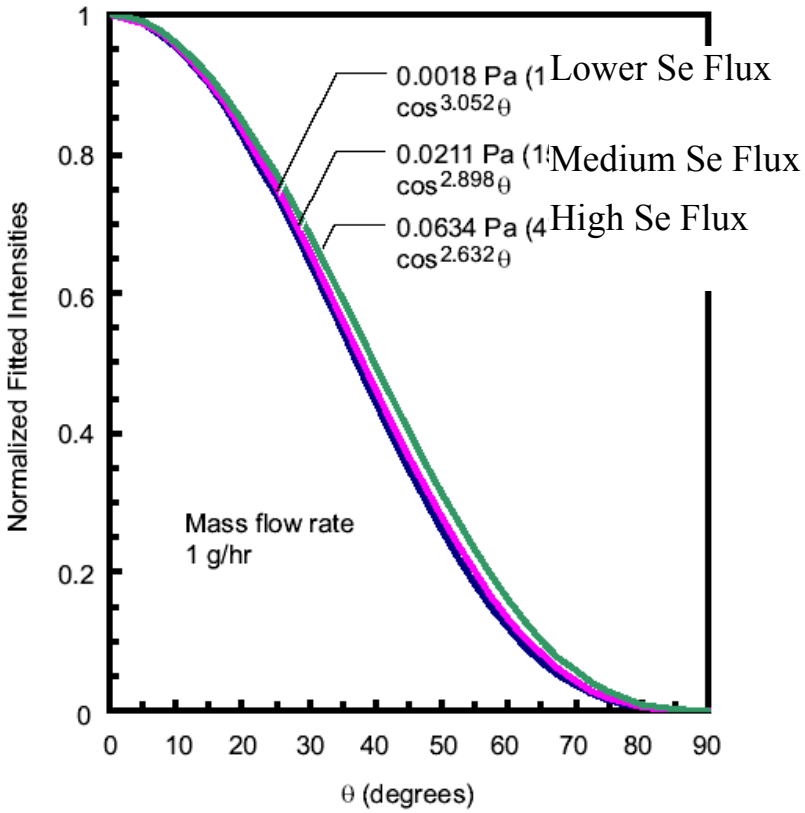

Figure 17. Normalized copper flux distributions for various selenium fluxes as predicted by DSMC modeling.

Deposition Model

Whereas the FE thermal model focused just on the effusion source, the deposition model (Figure 18) included the source, substrate heater, and the chamber walls. It evaluates the heat transfer to the web, including effusion source surroundings, reactor geometries, and web/heater assembly configurations. This model was created and analyzed using ABAQUS; results from the source models (FE thermal for Cu, Ga, and In) were simplified and applied as boundary conditions. Model results have provided insight to web heating changes with source outlet geometry changes, as well as an effective heater model to predict thermal gradients throughout the web.

When work started on the deposition model, it was found that the chamber was strongly affecting the source during start-up. To evaluate this, the reduced source model was first simulated with previous start-up production data (Figure 19).

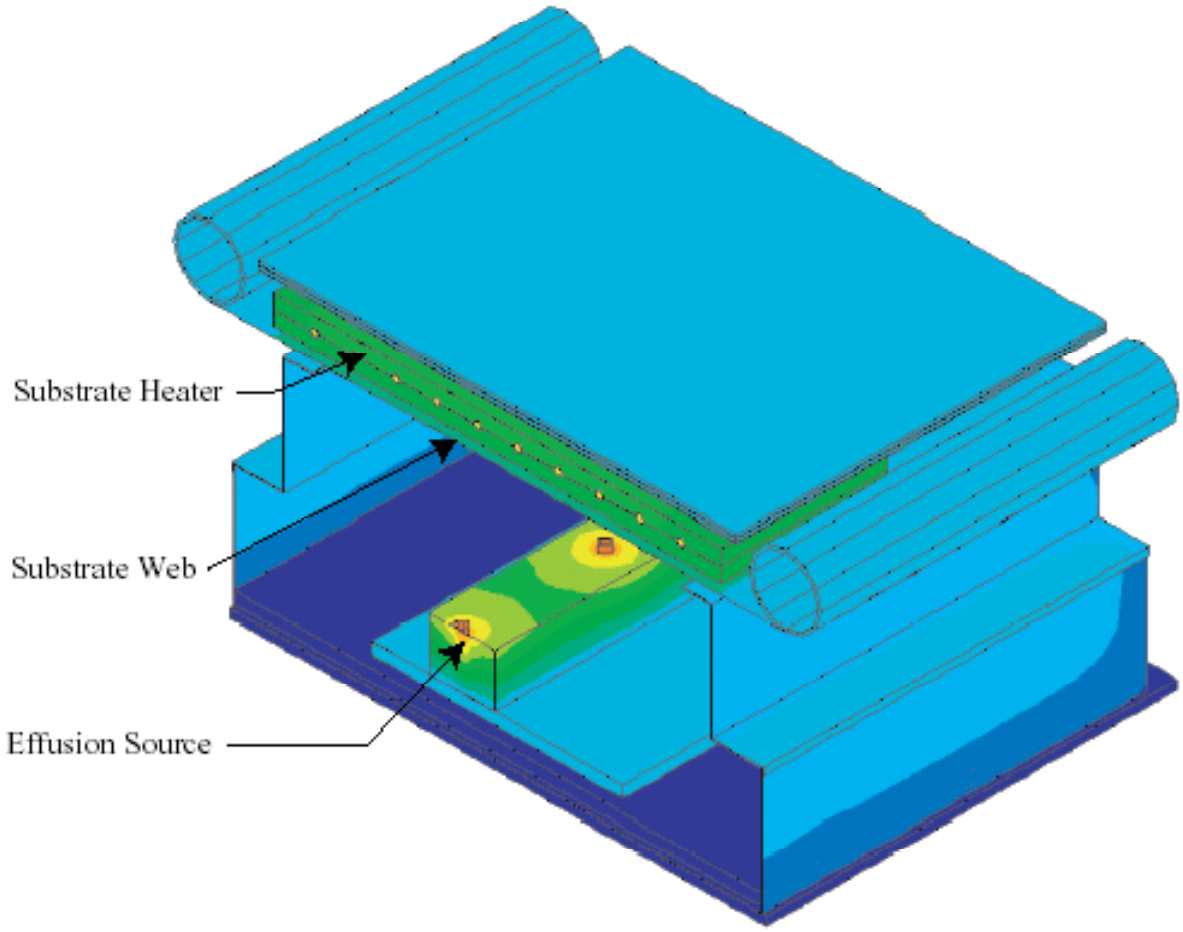

Figure 18. Schematic of Chamber Component used for the Deposition Model

The next step was to estimate the model between real power and the chamber output signal. Finally, to get the correct estimate of temperature during startup, the outputs from both the effusion source and the chamber source were added together (Figure 20). This combination produced a good estimate of the effusion source temperatures for start-up (Figure 21Figure).

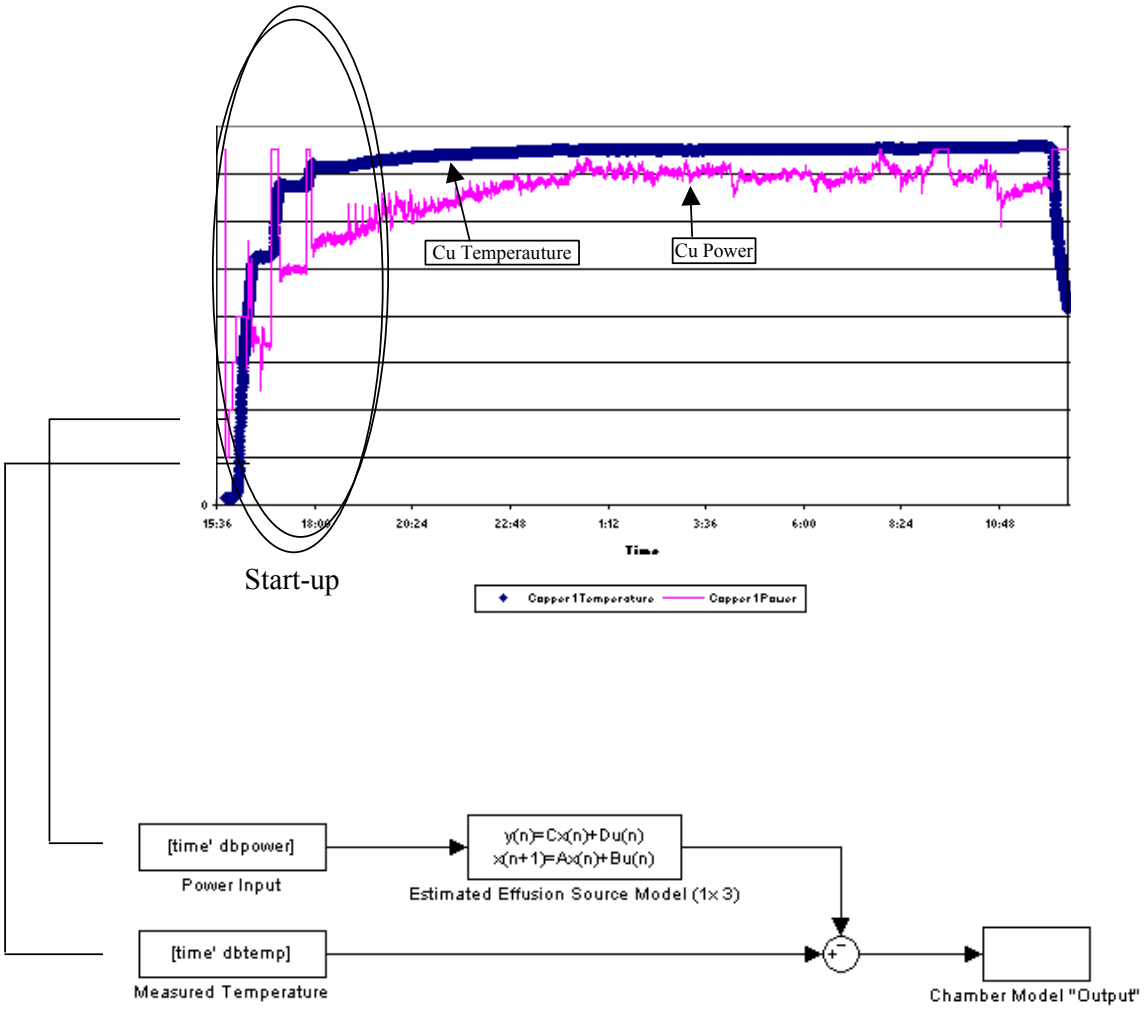

Figure 19. Schematic of Model Process used to Simulate Actual Deposition Chamber Output

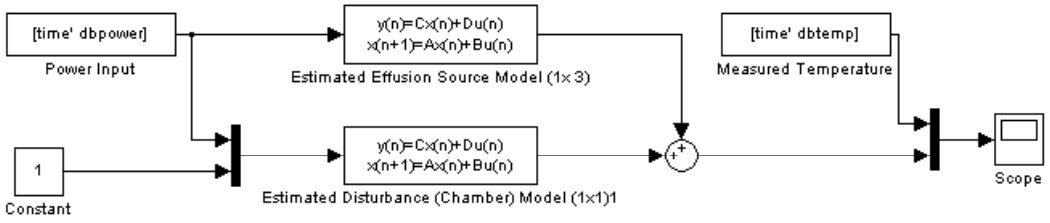

Figure 20. Schematic of model assimilation process

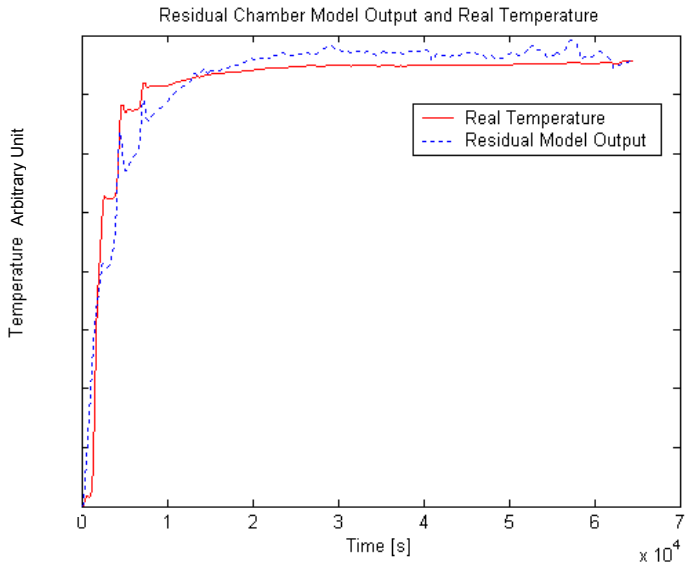

Figure 21. Comparison of predicted temperature and actual temperature

The steady-state temperature data from CIGS production runs were used to help fine tune inputs to the full ABAQUS deposition model. The model is validated with the results in Table 1, which are consistent with measured temperatures.

Table 1 – Comparison of predicted and actual temperatures.

TC Number	Description	Temperature Difference (Predicted - Measured Temperature)
1	Chill Plate (NOP side)	-16°C
2	Chill Plate (OP side)	6°C
3	Source Plate (NOP side)	1°C
4	Source Plate (OP side)	-8°C
5	Upper Cover, Take-up end	6°C, 1°C
6	Upper Cover, Pay-out end	2°C, -3°C
7	Source Plate	-10°C, -9°C
8	Upper Cover, NOP end	54°C, 27°C, 45°C
9	Upper Cover, OP end	-7°C, -2°C, 33°C
10	Se Source, top wall	Not in model
11	Se Source, inside Se melt	Not in model
12	Between Web and Substrate heater, Beginning of dep zone	44°C
13	Between Web and Substrate heater, Center of dep zone	0°C
14	Between Web and Substrate heater, End of dep zone	38°C

The model provided important information about the temperature gradients on the web. The web is about 200°C hotter above the source than when it enters the deposition zone (Figure 22). Across the web, there is an approximately 50°C change (Figure 23). Thus, this model enables improved uniformity, ability to determine CIGS processing temperatures, and dynamic control during warm-up or from large changes in processing. This may all be used to positively impact overall performance and yield.

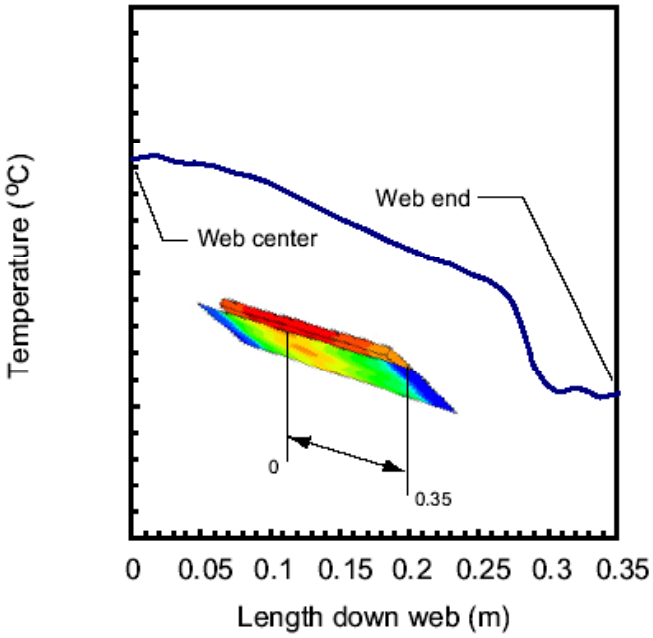

Figure 22. Variation of temperature along the length of the web at the web centerline

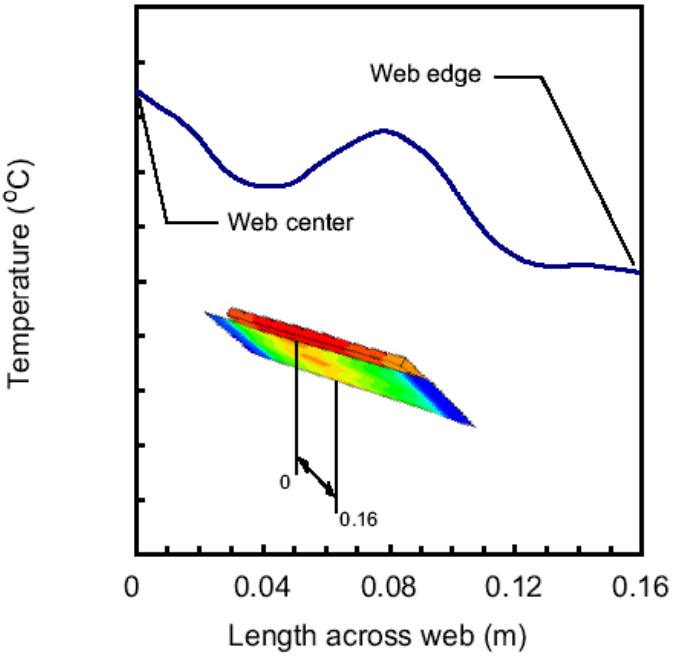

Figure 23. Variation of temperature along the width of the web from the centerline to the outer edge

2.1.2. ITO

The most important issue for ITO processing is a trade between conductivity and transparency, which are inversely related. To better understand the issues, physics based models were developed to associate power/efficiency losses related to the transparent conducting oxide (TCO) layer (in this case ITO). However, as part of the trade, aperture losses due to grid fingers, joule heating, dark distributed diode losses and shadowing must also be included to perform proper optimization. Basic models for each loss mechanism along with transmission and conductivity models for the ITO layer were combined and validated against data from production material (e.g. Figure 24). This model is used to provide appropriate processing targets for optimum ITO performance and is being continually compared to production-made ITO for evaluation purposes. Proper ITO optimization may provide 0.5 to 1% absolute efficiency improvement in PV device performance, while loss of proper control may significantly degrade overall performance.

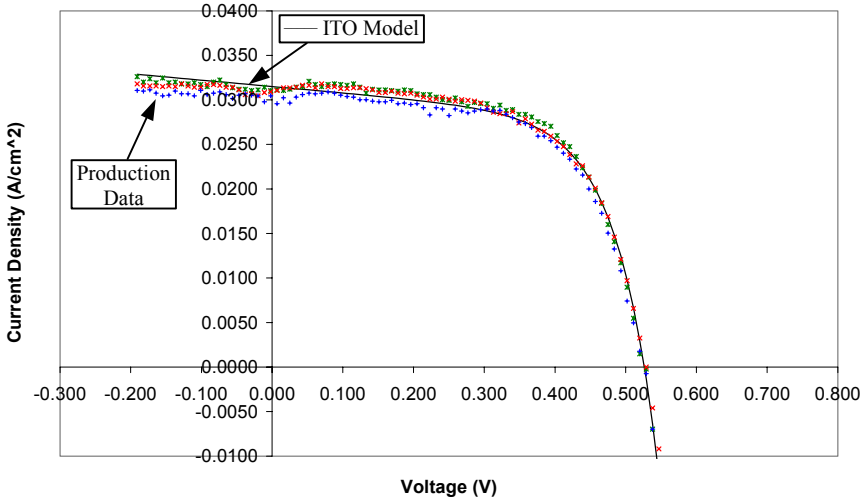

Figure 24. Small-area device J-V data along with a shunted ideal solar cell equation fit to the data.

2.2. Production CIGS PV Testing

As part of our production PV process evaluation, a systematic series of tests and analyses were performed comparing the different processed layers of production CIGS cells with "baselined" "research based" processed layers. The main goal was to determine any performance differences and potential improvements associated with the large area production CdS, ITO, and grid array processing along with the specific causes. In addition to standard I-V, QE, and spectral absorption analysis, samples are analyzed with XRD and spectroscopic ellipsometry. Typical testing involved completed CIGS PV cells (68.8 cm^2) cut into four equal sections (quarter cells) that were sufficiently small to fit into the characterization equipment. Direct comparison of performance was made with material that was pulled from the production processing before CdS and/or ITO deposition, along with completed material where one, two or three of the top layers was removed. All cells were finished with the research based processing and compared with the production material.

After thorough testing and analysis of the three layers on top of the CIGS absorber, the production step that was found most different between production and research based processing was the top current collection grid. The production system uses a silver paste as the top current collector where the research system uses a Ni/Al evaporated current collector. Measurements of the production grids showed hysteresis and unstable behavior in the dark and light JV characteristics when subjected to a reverse bias of more than –0.1 V (Figure 25). The behavior was evident when efficiencies were 8% or higher.

JV tests were performed on production material by sweeping from reverse to forward to reverse (RFR) forward to reverse to forward (FRF) for comparison. Large differences were observed depending on pre-

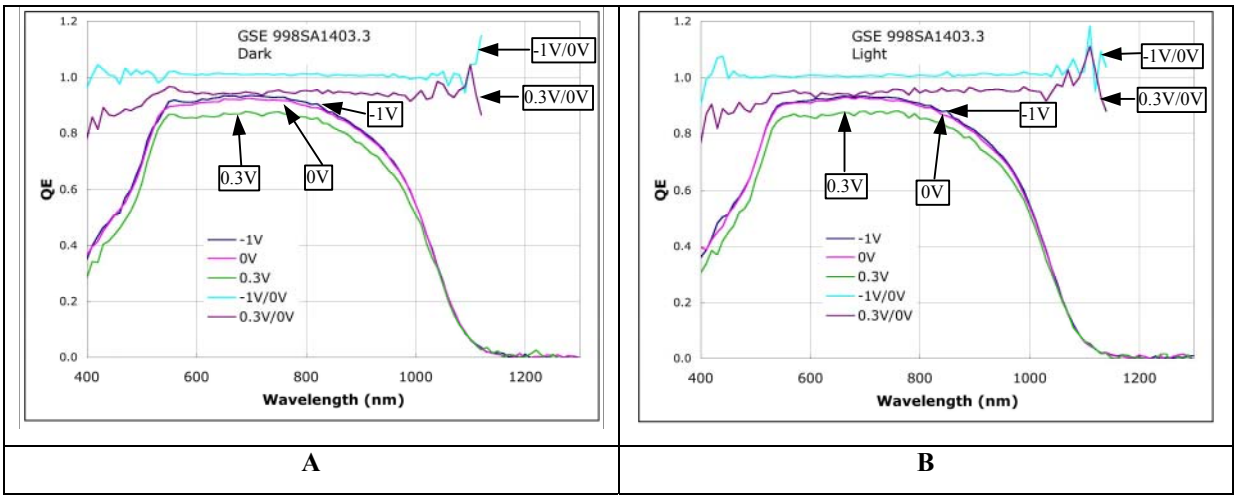

A B

Figure 25. QE data of a quarter cell at different voltage bias; (a) in the dark, (b) under 10mW/cm^2 ELH illumination.

test biasing conditions that were varied from –0.2V to -0.5V. Repeatability, stability and sweep dependence of the measurements were all issues. In general, FRF sweeps gave fill factors (FF) that were up to 10 to 15 percent lower, while Voc and Jsc were not significantly affected. In some cases FRF sweeps resulted in very unstable JV characteristics that recovered to a certain degree after forward bias light soaking (Figure 26). Also, cell efficiencies improved more than 15% when the current collector was changed from the silver-paste (production) to the evaporated Ni/Al grid (research). While the specific mechanism for the significant difference is still being determined, the research clearly identifies a potential area for improved performance and also indicates that the other production processes are performing adequately. The most significant loss mechanism, excluding current collector grids, of the production-completed devices was in the series resistance, lowering the fill factor, due to ZnO/ITO layers. Other than that devices completed with the research reactors are no different than the devices from the production reactors.

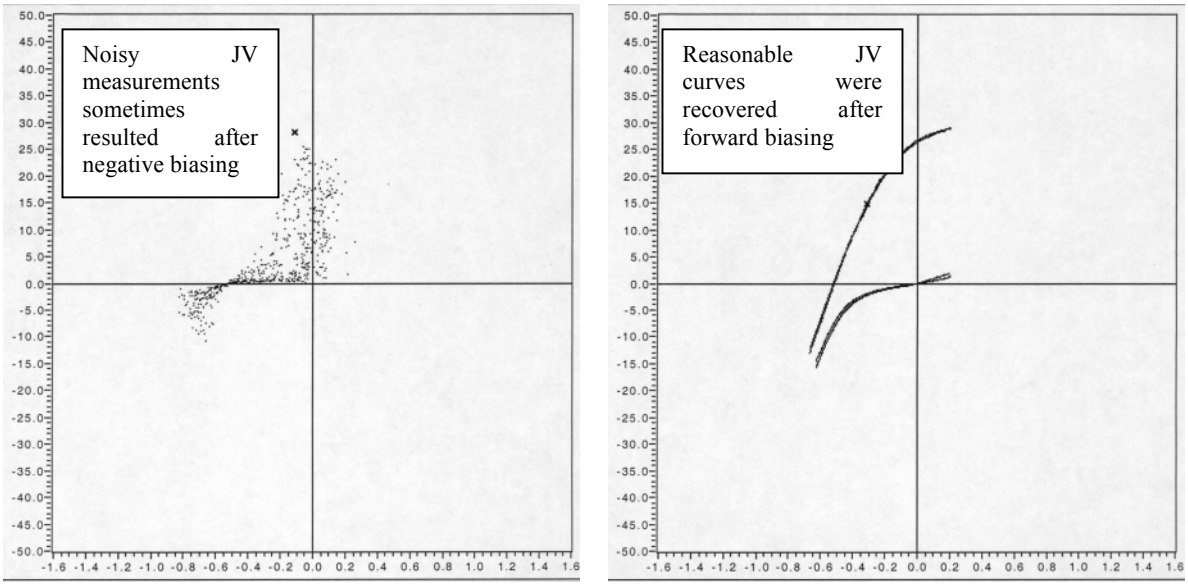

Figure 26. JV test results of forward, reverse, and forward sweeps of production CIGS cells. After reverse biasing, some of the cells resulted in very noisy JV curves (Left). However, some of the samples were recovered and produced good JV curves (Right) after 30 minutes light soaking at +0.6V (FRF sweep).

CIGS PV Cell Characterization

Variable Angle Spectral Ellipsometric (VASE) analyses was performed. The multi-layer film structures that gave the best fit to data did not match the qualitatively different Ga profiles. That is, for some of the samples the model showed a Ga rich surface layer while for others Ga content decreased monotonically from the Mo interface to the free surface. The fitting algorithm assumes knowledge of optical properties as a function of Ga content. For $CuInGaSe_2$ the reference sample had a Cu/(Ga+In) ratio of 0.9. If there were variances in this ratio from one edge to the other, they might affect the "best fit" obtained from the fitting software. Data were obtained for the numbered coupons labeled in Figure 27. Figure 28 shows representative VASE data along with corresponding model fits that are used to determine the structure (e.g. thicknesses) of the component films. To obtain appropriate fits to the data and keep the fitting computation time reasonable, the following assumptions were used in the models:

- Surface roughness and intermix layer are of the same thickness, except for $CuInGaSe_2$/CdS which was assumed to be 50% higher,
- Intermix layers are modeled as an equal mixture of materials in contact,
- Ga content in the $CuInGaSe_2$ film decreases from the Mo interface into the film, goes through a minimum then increases at the surface.
- The major conclusion from the spectroscopic ellipsometry analysis of the numbered sections is that coupon 5-3 had a significantly thicker oxide layer thickness, compared to the other coupons. This is a little unexpected since substantial color difference are observed and are probably due to CdS thickness variations. Repeated data analysis using different CdS reference data provided no major differences in the results.

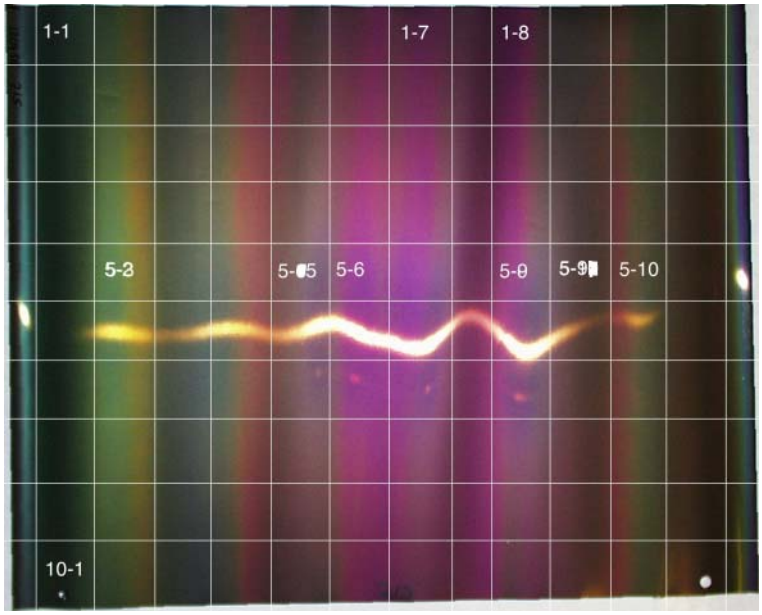

Figure 27. Photograph of representative production CIGS PV cell material demonstrating the easily observed color variations through the sample. The cell is divided into 1" X 1" sections for comparative analysis. Specific numbered sections were analyzed with spectroscopic ellipsometry.

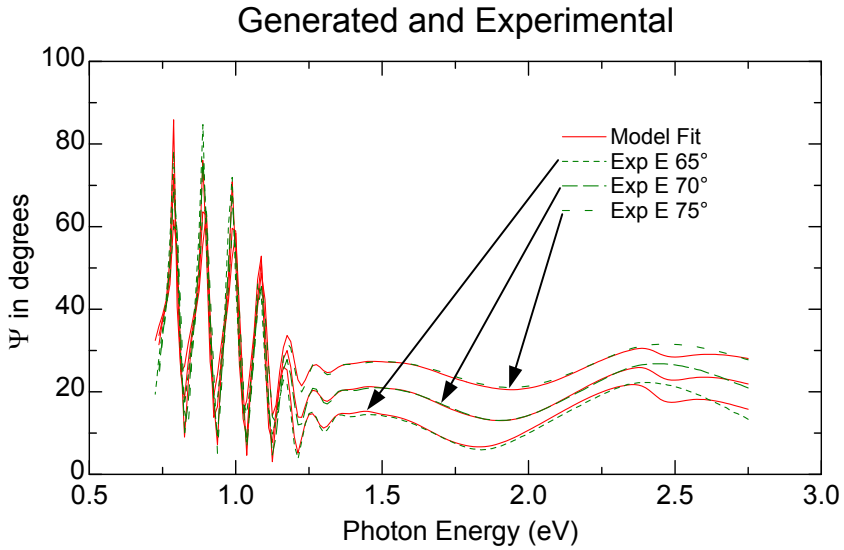

Figure 28. Representative comparison of experimentally measured VASE data and calculated model fits.

3. Reliability: Fault Prevention and Fault Tolerance

System reliability has been improved by fault prevention and fault tolerance. Fault prevention is always a high priority, and includes operator interlocks and training, routine inspections of equipment, and use of a preventative maintenance schedule to replace parts before a fault occurs. Fault tolerance work on the CIGS process, including Cu, In, Ga, Se, and Na sources, is discussed below.

3.1. Cu, In, and Ga

Decision-making algorithms were designed as part of fault-tolerant strategies for various controllers. Results generated by the fault-detection algorithms determine when faults have occurred. However, for example, an abrupt change in the temperature measurement is not necessarily a faulty thermocouple (Figure 29). Thus when a fault is detected, a comparison is made with a second measurement to ensure that the thermocouple is actually faulty. When a thermocouple is deemed to have failed control is switched to a second (redundant fault tolerance) thermocouple or for indium and gallium control is switched to control based on source input power.

For the copper effusion source the control is more complex. In this case two controllers are designed to control the effusion rate of copper. In the primary controller, thermocouple and XRF measurements are used in the feedback loop. In the secondary controller, input source power set points are controlled by XRF measurements. Initial development of this latter controller has demonstrated the potential for power/XRF based control. However additional development and validation is required.

The reduced models presented in 3.1.1 may be helpful in a power/XRF based control loop. Figure 30 is a block diagram of the control loop with the thermal model directly replacing the source thermocouple. This is the simplest implementation and use of the thermal model. Every time the power is sampled, the thermal model calculates a new temperature. This temperature is compared to the estimator temperature and the controller adjusts the power appropriately. Additional activities to determine the usefulness of this approach will be performed. Full implementation of redundant source thermocouple, fault detection and fault recovery for CIGS source control should provide improved yield and throughput by preventing system upset due to a faulty sensor and system shutdown once the sensor is identified as defective.

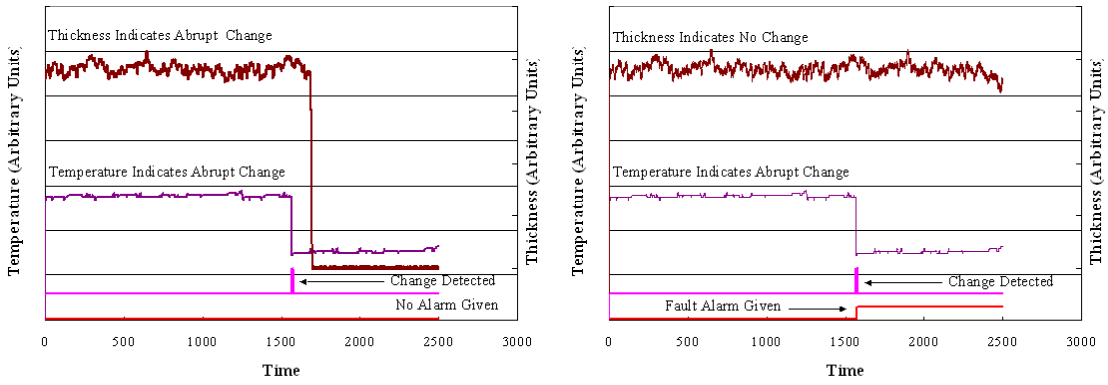

Figure 29. Example of fault detection process – An abrupt change in temperature measurement is not a thermocouple fault (left) and (2) is a thermocouple fault (right)

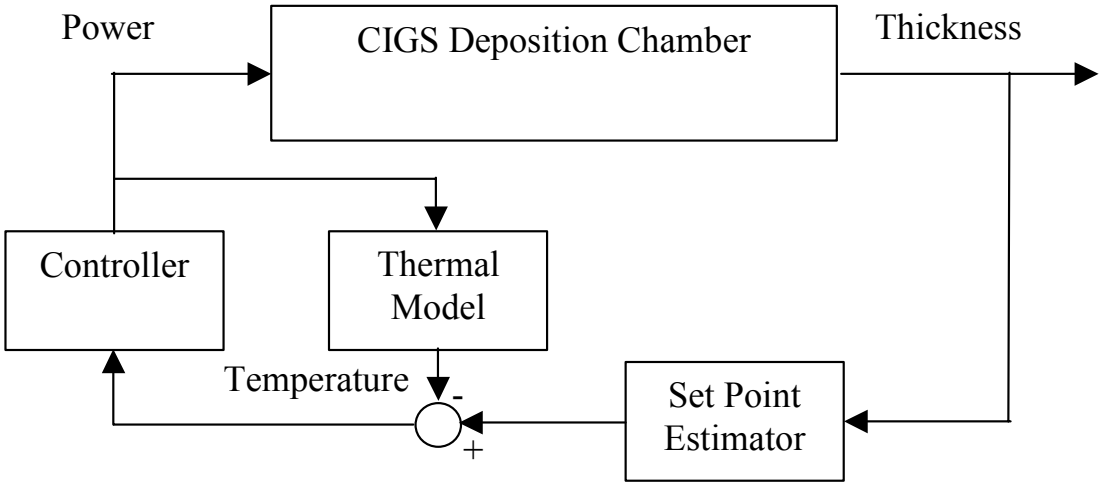

Figure 30. Potential control loop using reduced thermal model

3.2. NaF

Control of NaF delivery and thickness is important for adhesion and efficiency. Since direct thickness control is presently not available, delivery control based on flux measurements has been determined to provide superior control compared to that of source temperature. However, flux sensor failure occurs fairly frequently and unpredictably. Thus, a decision-making algorithm was developed to compare measured flux sensor noise with predictive models for the sensor response based on source temperature measurements. Once the flux monitor becomes too noisy (Figure 31), sodium fluoride control is switched from flux based to thermocouple control. Initially, the NaF fault tolerant system used a one-fault detection algorithm. That is, once a fault was detected, the supervisory control loop was disabled and the low-level control loop was left unchanged. Subsequent data evaluation indicated that temporary faults were occurring, i.e. sometimes the NaF measurement returned to a normal state after a faulty event. Therefore, the fault tolerant algorithm was modified to "reset" if the NaF measurement returned to normal and re-engage the flux based supervisory control loop. Initial results indicate the fault tolerant strategy is operating as designed, to eliminate process upsets, and thus improve yields, due to faulty flux sensors and yet enable superior module performance through better control of NaF thickness.

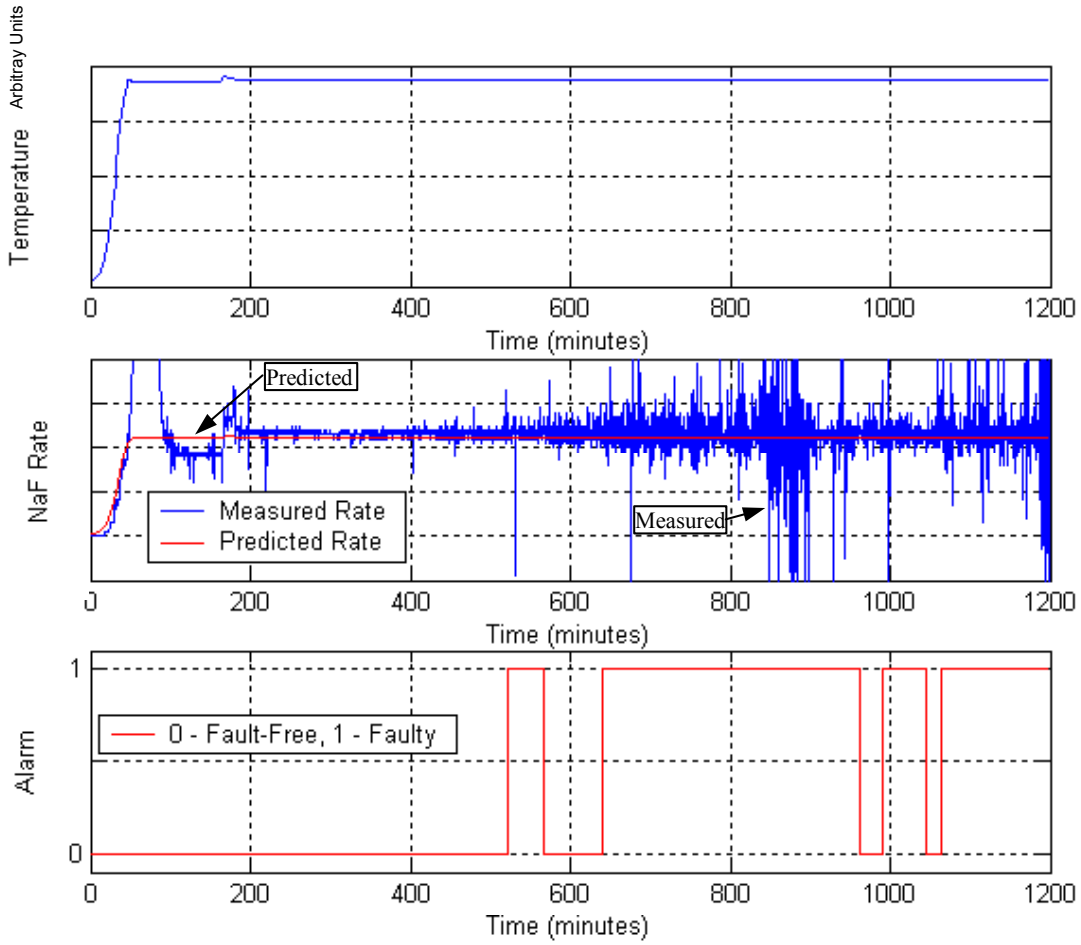

Figure 31. Comparison between measured NaF flux and a predictive model is used to determine when the sensor is faulty. Based on a prescribed set of conditions, when the sensor is determined to be faulty, an alarm is enabled and the supervisor control switches to a fault recovery strategy using NaF source temperature for control.

3.3. Se

Se fault tolerance is similar to that of NaF fault tolerance procedures. Again, control based on Se flux has been demonstrated to be far superior to that of source temperature/power. However, unanticipated process upsets occur where the flux sensor goes out of range, thus not providing useful measurements for control. A fault-detection algorithm was then developed to identify these large spikes in signal, leading to an alarm. A decision-making algorithm causes the sensor to turn off and temporarily switches to constant source power control to eliminate out-of-bounds Se delivery and thus preserve CIGS yield and performance. The Se sensor is then probed at set intervals to determine if it has recovered. Se flux sensor control is reinstated when it is recovered (Figure 32) to provide optimum CIGS module performance.

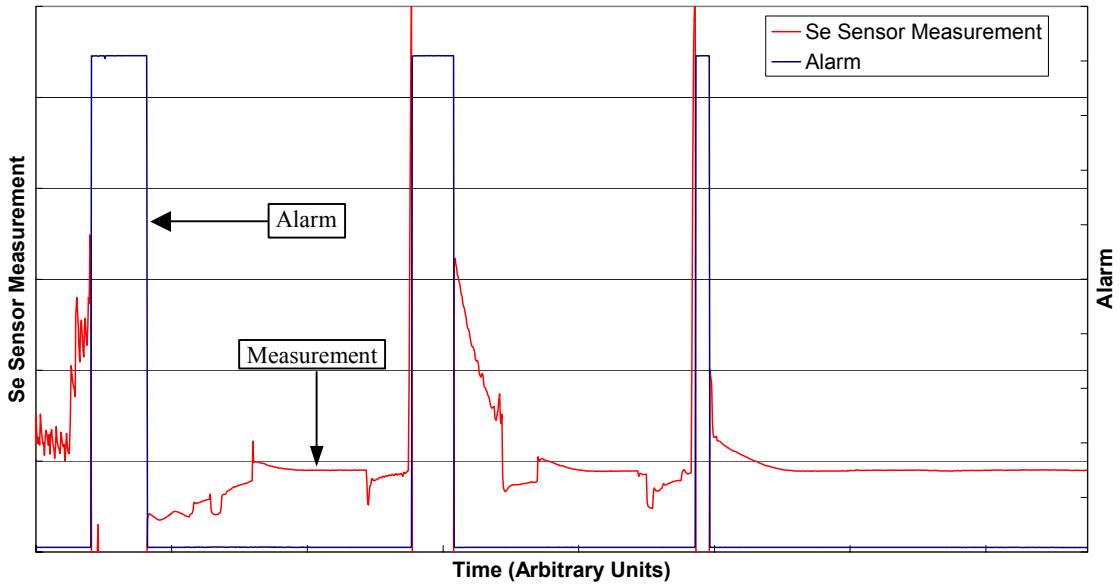

Figure 32. Se fault tolerance showing large spikes leading to an alarm and constant power control. Once the sensor is recovered, Se sensor control is reinstated.

3.4. ITO

As part of the overall control strategy for ITO, two components of model development were integrated into production systems; target wear and conductivity versus transmissivity. To ensure proper thickness control of the sputtered film for optimum PV device performance, target wear must be accurately accounted. Compensation algorithms were developed and implemented on all ITO chambers. These algorithms compensate for the amount of deposition from each target and provide power set points to each target power supply at any given time:

$$PowerSP_{next} = PowerSP_{start} + k \times KWH_{total}$$

where $PowerSP_{start}$ is the power set point when the target is new, k is the set point stepping value, and KWH_{total} is the total energy consumed by the target since it was installed. $PowerSP_{start}$ and k values were validated against production data. It has been found that k = 2.6877 for ITO and 2.3253 for Mo systems. This technique has been working well towards obtaining desired Mo and ITO film thickness in production.

4. Sensors

Sensor development is at the core of the process control efforts. In-situ sensors can be used to provide direct feedback control or be used as part of fault tolerance. The numerous sensors being developed are in various stages, from testing on the bench-top to integral components for process control activities on production deposition systems.

4.1. CIGS

CIGS, because of the complexities of the process as well as the variety of materials deposited, has been a key area for sensor development. Combining these sensors with process control and fault tolerance strategies has provided significant increases in CIGS quality and consistency.

4.1.1. Emissometer

A commercial emissiometer that provides in-situ temperature, emissivity, and surface roughness measurements of the CIGS absorber layer has been procured and tested both in CIGS deposition systems and on the bench-top. Due to the tremendous value such information could provide for process control and in-situ film evaluation, efforts to overcome several integration issues associated with alignment sensitivity and hardware temperature limitations have been deemed to be worthwhile. Based on initial vacuum chamber and bench top testing, the procured system was upgraded to provide better measurements. Initial evaluations of the upgraded system using polished silicon wafers with known emissivities are shown in Figure 33. The instrument performed better and tracked temperature changes but demonstrated too much temperature dependence for the emissivity and the temperature calibration was an issue. More development efforts will be performed to optimize and calibrate the emissometer.

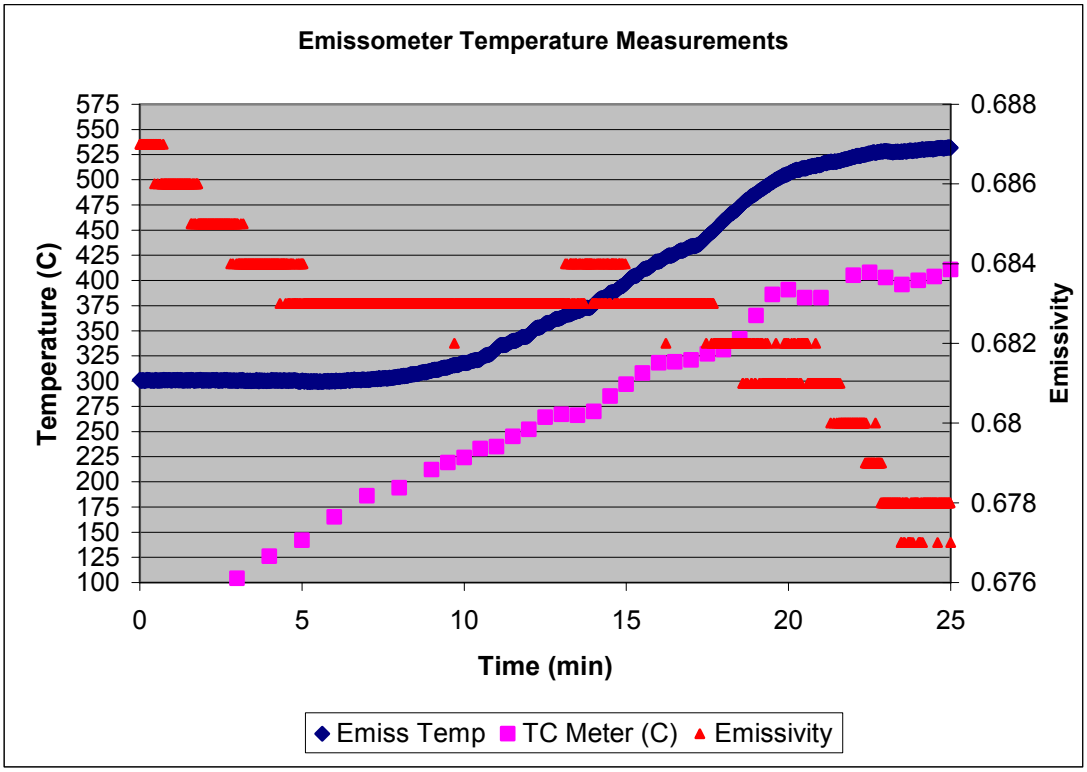

Figure 33. Emissometer temperature and emissivity measurements of a Si wafer compared to temperature measurements from a thermocouple.

4.1.2. In-situ Pyrometry

Substrate temperature during CIGS deposition processes is a very important parameter for high performance devices that has not been accurately measured and controlled. Standard techniques for mounting thermocouples on the substrate provides limited information since thermal mass of the substrate, emissivity of the films, and thermal conductivity issues with the thermocouple all affect the measurement. Furthermore, thermocouples in the substrate or on the backside of the substrate do not directly measure the temperature of the CIGS film itself. Finally, embedded thermocouples are physically impossible with a moving flexible roll-to-roll substrate.

Optical emission measurements of the CIGS film may provide accurate temperature data, however, implementation in the harsh Se containing CIGS deposition environment, the relatively low substrate temperature, and the CIGS optical properties can all detrimentally affect the measurement. Our substantial expertise with incorporating optical fiber based sensors in CIGS deposition systems was

leveraged to design and construct an optical probe that reliably collects the emission from the CIGS film on moving vibrating flexible substrates. This collected signal is then analyzed with a spectrometer and fit using standard physics equations to determine the CIGS film temperature.

Initial measurements indicate that sufficient emission signal (Figure 34) is available at standard substrate processing temperatures to provide reasonably accurate temperature measurements. Several issues must be adequately addressed before a robust and accurate CIGS film temperature measurement can be made in-situ and in real-time on a moving web. These issues include:

- Wavelength region used to perform the temperature measurement. Shorter wavelengths above the CIGS band gap have less signal and thus inherently more inaccuracy. However, longer wavelengths below the band gap have higher signal intensities but may have interference fringes. It may be possible to choose a wavelength range where both can be measured simultaneously and thus temperature; optical properties and film thickness can be determined.
- Signal to noise is paramount to accurate temperature determination. Sophisticated analysis methodologies were implemented that automatically determines the functional usability of the collected signal and thus the temperature. Initially, statistical comparisons between the actual signal and the theoretical curve shape should provide this key determination.
- Due to the wavelength variability of the optical fibers and spectrometers, a calibration methodology was developed that predetermines the wavelength dependence of the detection hardware so that an accurate emission spectrum can be obtained. This calibration used a black body oven with known temperatures.
- Wavelength dependent emissivity changes as a function of temperature can adversely affect the temperature determination. Systematic methodologies based on comparison with theory can be employed to detect and adjust for these wavelength dependent emissivity changes. Furthermore, for CIGS films, these types of effects are not expected to be significant.

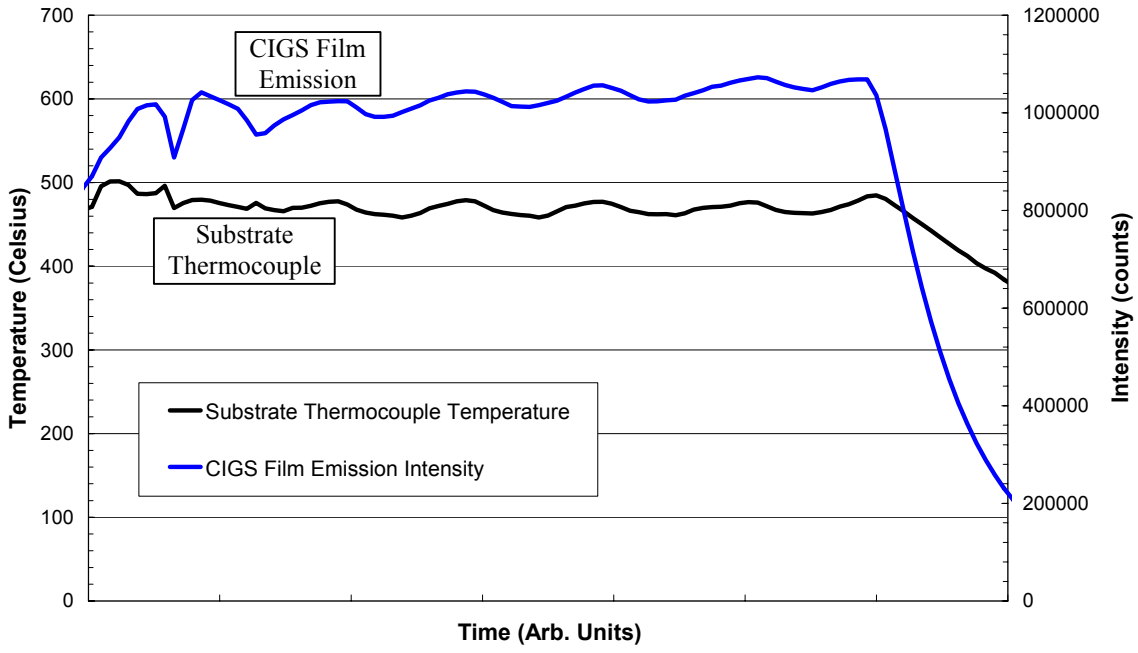

Figure 34. Measurement of emission intensity from CIGS films at nominal substrate operating temperature

The main advantages to our approach are that the measurement is emissivity, sample distance, and intensity independent. This is a tremendous help for performing measurements in a Se containing environment where the CIGS film emissivity changes substantially with small changes in composition and the substrate is constantly moving. Thus, even though changes in material composition will significantly change emissivity and thus the actual temperature of the CIGS film, our technique will accurately measure these changes.

Initial in-situ real-time substrate temperature measurements correlated well with thermocouple readings from the substrate heaters and on the sheath surrounding the optical probe). A formula was developed that used intensity normalized by temperature to the 4th power and error normalized by intensity to evaluate the accuracy of the optical temperature measurements. This analysis unambiguously determined when sufficient signal to noise was available to provide reasonable temperature measurements (as indicated by the "selected temperature" data shown in Figure 35). Typically, the optical temperature measurements were deemed to be acceptable above ~ 350°C, but since the specific film properties significantly affected this "threshold" autonomous real-time calculations are used to provide acceptability determination for every data point.

As shown in Figure 35, measurements from a thermocouple in the vicinity of the substrate were also measured. A series of experiments were conducted in which the properties of the substrate were studied to determine how substrate temperature and tension affected cracking of the thin-film of molybdenum deposited on the substrate. As shown in Figure 35c, significant changes in emissivity (i.e. from CIGS to bare stainless at the end of the deposition) results in less radiated heat from the web decreasing the measured temperature by the thermocouple but a higher substrate temperature as measured by the IR spectrometer. Further experiments and calculations will be performed to investigate and fully characterize this phenomenon. In addition, experiments were conducted to investigate the thermal properties of the transition from Cu rich (Cu/(In+Ga) >1) to Cu poor (Cu/(In+Ga) < 1) CIGS indicating an inverse correlation between Intensity/T^4 and the Cu ratio. Overall, the IR spectrometer based pyrometer has been demonstrated to provide reliable in-situ real-time substrate temperature measurements.

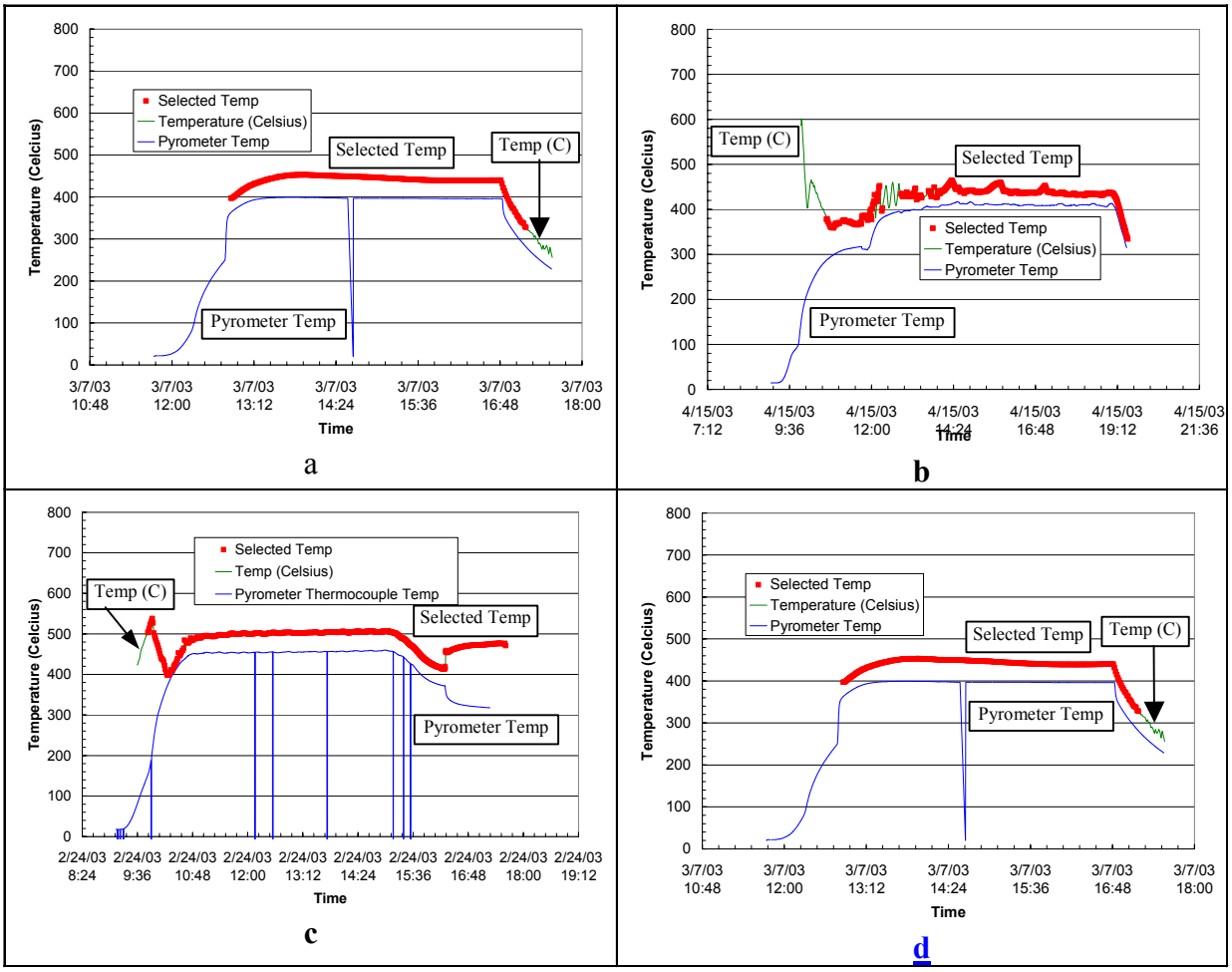

Figure 35. In-situ real-time CIGS deposited film temperatures measured with IR spectroscopy. The data marked as "pyrometer Temp." is based on measurements from a thermocouple attached to the insulation of the fiber optic (approximately ¼" from the web) used to collect the light emission from the heated web. The data marked as Temp (C) were converted using a calibrated instrument matrix from spectral emissivity measurements collected from the heated web. The data marked as "selected temp" are spectral emissivity based temperature measurements where comparison to Intensity T^4 has determined that the temperature accuracies are within acceptable limits. The data indicate that compared to a thermocouple ("Pyrometer Temp") placed close to the flexible substrate, the CIGS film temperature was higher and not accurately represented by the thermocouple during non-equalibrium conditions or where the emissivity of the thin-film changed significantly (end of run in c).

4.2. ITO and Mo

Based on activities in Phase I, sensor integration activities for the sputter deposition systems in Phase II included:

- Residual gas analyzer (RGA) to monitor process off- gas composition,
- Optical emission spectrometer (OES) to monitor plasma composition,
- Input source power monitoring/control for fault tolerance, and
- In-situ ITO resistance monitoring for process control.

In addition to potentially improved control of ITO sheet resistance and optical transmission properties to enhance overall module performance, implementation of these sensors may provide in-situ health monitoring of the deposition processes to improve yield and performance through the detection of unanticipated process upsets and by identifying additional day-to-day fluctuations in the manufacturing.

RGA

Extended-pressure RGA monitoring was installed on production ITO and Mo deposition chambers. RGA provides monitoring of the reactive and/or residual gas partial pressures over the entire run for system health and control. For example, RGA was instrumental in detecting a leak in an Ar feed line. The leak detrimentally affected deposited Mo film quality, which was corrected once the leak was addressed. Figure 36 shows representative data of peak intensities of several molecules from an RGA sensor on an ITO deposition system. General agreement between RGA and simultaneous OES process data was good (at least semi-quantitatively) for those chemical species quantifiable by both techniques.

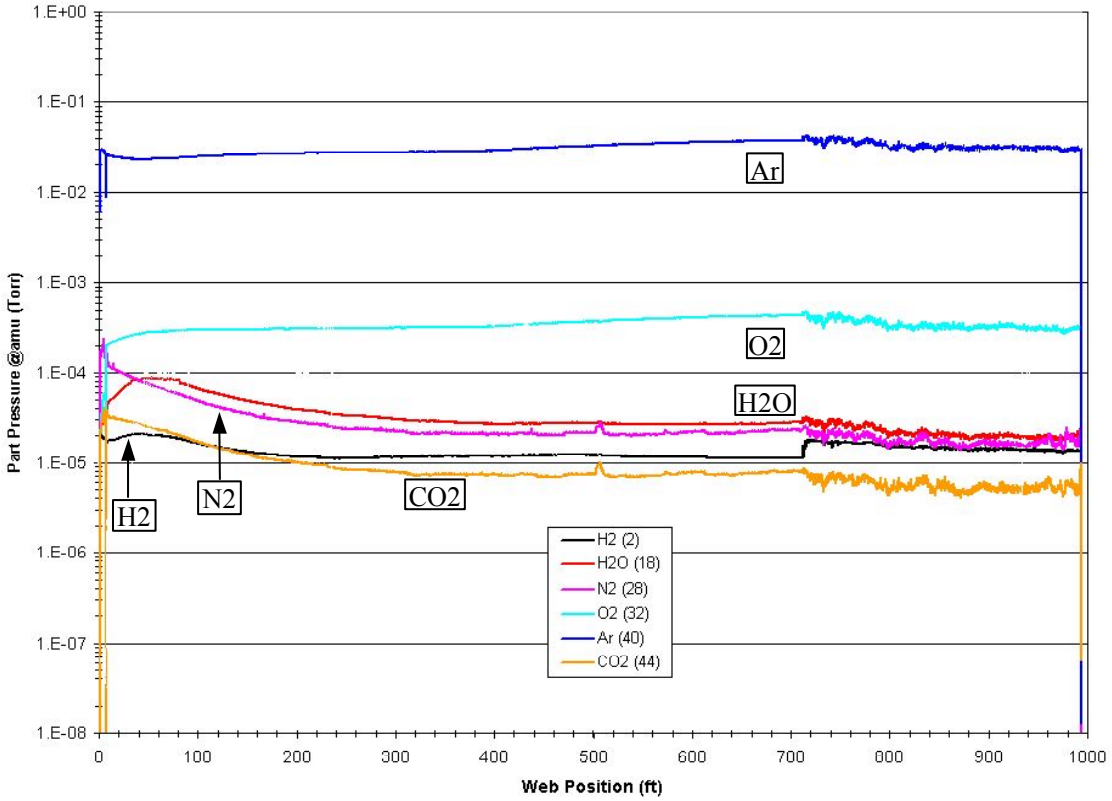

Figure 36. Representative RGA data from ITO production deposition. The series represent peak intensities during the production run.

OES

OES provides direct measurement of the ionic composition of the sputtering plasma which can be used for health monitoring and process control. Initial testing proceeded on production ITO chambers with installation and data collection. Probe optics and optical fiber were fixtured to sample across the widths of the targets for optimum signal collection. Spectra were obtained every 30s throughout the course of each deposition cycle for several production runs. The software also logged (in a separate file) instantaneous intensities for Zn, O, Ar, N, OH. Analysis of ZnO emission data from these production runs suggests a change in the surface stoichiometry of the ZnO targets at the sputter conditions now in use.

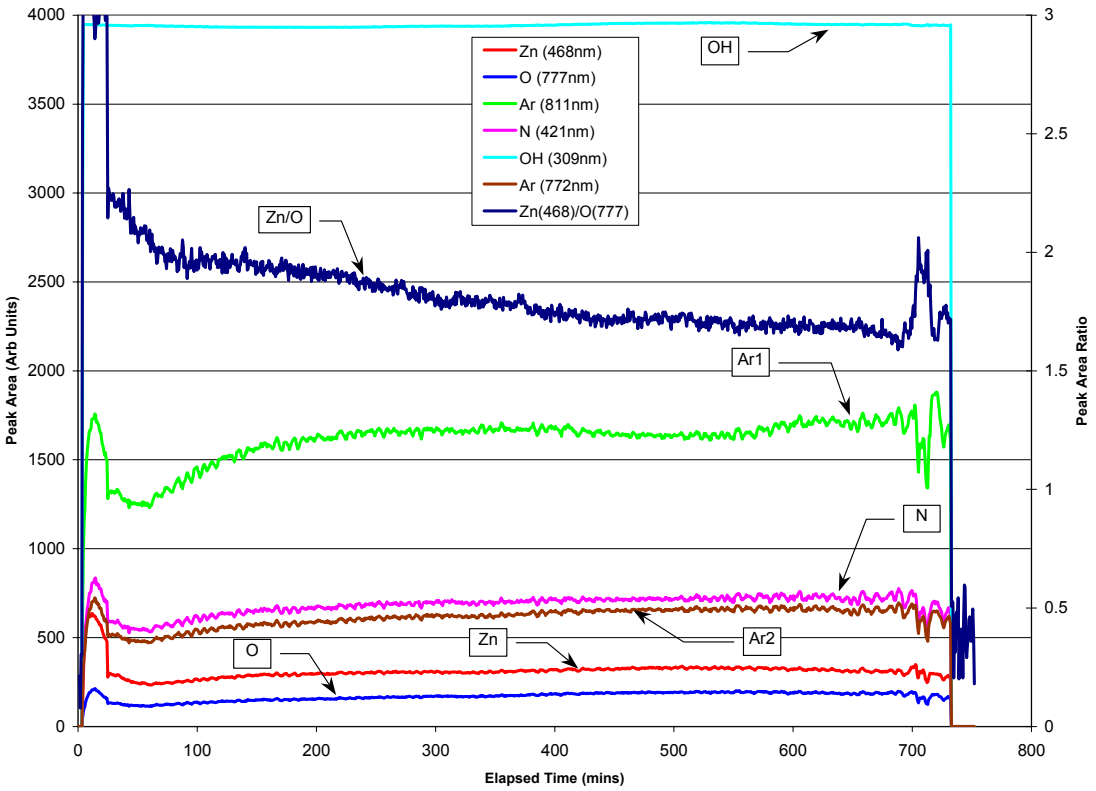

Figure 37. Representative OES data from ZnO production deposition.

As an example, in production, ITO sheet resistance increases with time during the deposition runs (Figure 39). The RGA and OES (Figure 38) correlated this observation with both steadily increasing O_2 partial pressure and steadily decreasing H_2O background. These results have identified a potential source for the observed resistance increase and a potential for process control. To improve PV module performance through ITO optimization, future experiments involving off-gas and plasma monitoring to develop quantitative correlations and active feedback control mechanisms will be developed. This will include experiments involving step responses and correlated OES/RGA signal changes of specific feed gasses to determine their potential for process control.

In-situ Resistance Probe

Based on current knowledge and expertise, an in-situ probe was developed to monitor the change in sheet resistance of deposited ITO, which leads to variations in cell efficiency. This probe enabled real-time resistance measurements. Representative data are presented in Figure 39 demonstrating that the sheet resistance varies significantly over the course of a production run. Also plotted in Figure 39, are ex-situ sheet resistance measurements, which correlate well with the in-situ data. The data indicate that the in-situ resistance measurement may provide acceptable measurements for real-time process control once an appropriate control strategy is identified and implemented.

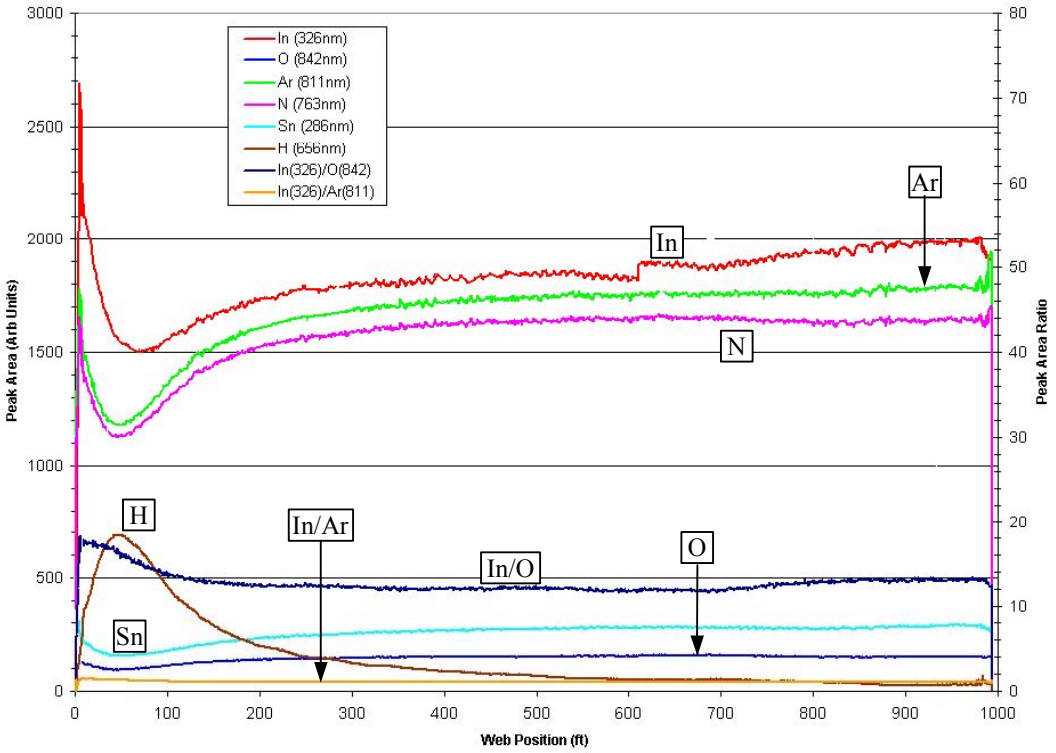

Figure 38. Representative OES data from ITO production deposition.

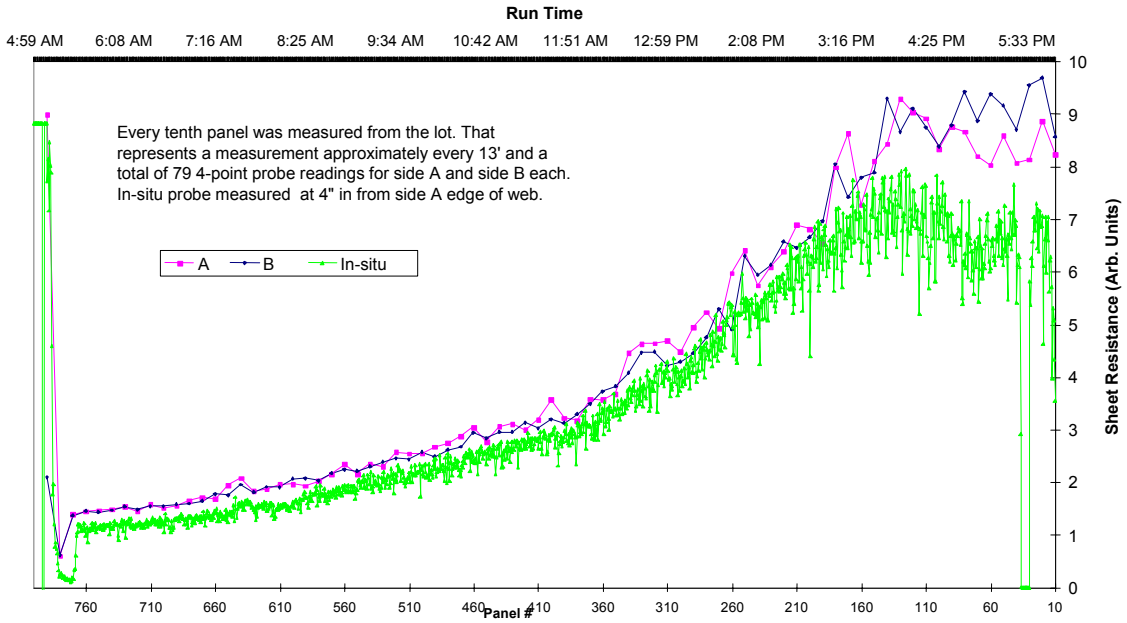

Figure 39. Representative data from in-situ resistance measurements. Ex-situ measurements (dark and light blue) are comparable to the in-situ (green) measurements.

CONCLUSION

ITN and GSE with the assistance of NREL's PV Manufacturing R&D program are continuing to advance flexible CIGS production technology through a multidisciplinary approach focused on substantial improvements in thin-film deposition processing. To date, progress has been made in several areas, including:

- The design and implementation of trajectory oriented physics-based control models on production deposition systems to provide improved dynamic control, systems design, and fault tolerance. Comprehensive physics-based deposition system models have been completed to enable overall system design evaluations and high fidelity process control. These models have been used to develop improved metal deposition sources, to investigate improved start-up control and for other process related issues. In addition, model reduction strategies have been developed to provide algorithms that can be used for real-time feedback control.
- Fault tolerance strategies have been evaluated, identified and in some cases implemented for production deposition systems. These activities include detection of faulty sensors (e.g. Se, Na, sputter targets, thermocouples, etc.), fault mitigation through autorestart (e.g. Se, Na, sputter targets, etc.), and fault recovery by automatically switching to alternative control/processing strategies that enable continued processing, thus eliminating the time and high costs associated with run termination.
- Development and in some cases implementation of additional robust in-situ sensors to provide real-time process and product information for feedback and feed forward control. Development activities included source, flux and thin-film property sensors to provide the most appropriate information for the best control possible.

These Phase II activities have resulted in outstanding improvements in CIGS cell performance (>10% average) and yields (>90%), while substantially reducing fault events due to component/system breakage. These gains have primarily been due to improved process parameters identified through systematic evaluation that was enabled by the improved control provided by the PV Manufacturing R&D program activities. In Phase III, activities that build upon these tremendous accomplishments will be performed to complete several process control and fault tolerance tasks and implement additional process improvements.

ACKNOWLEDGEMENTS

The authors gratefully acknowledge and thank UniSource Energy Corporation and the Department of Energy's National Renewable Energy Laboratory, Photovoltaic Manufacturing Technology Program, Contract Number DE-ZDO-2-30628-07, for their support. We would also like to thank all the people who have contributed to the success of the program including Lin Simpson, Nick Gomez, Bharat Joshi, Greg Kleen, Garth Jensen and Kevin Williams at ITN Energy Systems, Inc.; Scott Wiedeman, Jeff Britt, Jane VanAlsburg-Westermann, Marcus Beck, Jim Taylor, John Muha, Eric Sheehan, Bob Huntington, Doug Mason, and Omran Musbah at Global Solar Energy, Inc.; Tyrone Vincent, J.P. Delplanque, Robert Key, Jeff Hanna, and Matt Hilt at the Colorado School of Mines; and Erten Eser, Robert Birkmire, and William Shafarman at the Institute of Energy Conversion, University of Delaware, DE.

REFERENCES

[i] Hanna, Jeffrey, "Finite-Element Modeling of Thermal Behavior found in High-Rate Metal Vapor Effusion Sources and a Multiphase Flow Model of Particle Formation and Growth in the Metal Vapors," Colorado School of Mines

[ii] R. J. Kee, F. M. Rupley, J. A. Miller, "Chemkin-II: A fortran chemical kinetics package for the analysis of gas-phase chemical kinetics," Report SAND89-8009/UC-401, Sandia National Laboratory (March 1991)

[iii] DS2V software by G.A. Bird (G.A. Bird, *Molecular Gas Dynamics and the Direct Simulation of Gas Flows,* (Clarendon, Oxford, 1994)

[iv] Hilt, Matthew J., “Validation and Reduction of Models for High Rate Metal Vapor Effusion Sources,” Colorado School of Mines

[v] Kodas, Toivo T. and Hampden-Smith, M., Aerosol Processing of Materials, Chapterts. 4 and 5, "Particle Growth, Evaporation, and Nucleation" and "Collision and Coalescence," pp. 75-128.

REPORT DOCUMENTATION PAGE

Form Approved
OMB No. 0704-0188

PLEASE DO NOT RETURN YOUR FORM TO THE ABOVE ORGANIZATION.

1. REPORT DATE *(DD-MM-YYYY)*	2. REPORT TYPE	3. DATES COVERED *(From - To)*
November 2004	Phase II, Annual Technical Report	March 2004

4. TITLE AND SUBTITLE
Trajectory Oriented and Fault Tolerant Based Intelligent Process Control for Flexible CIGS PV Module Manufacturing Scale-Up, Phase II, Annual Technical Report, March 2004

5a. CONTRACT NUMBER
DE-AC36-99-GO10337

5b. GRANT NUMBER

5c. PROGRAM ELEMENT NUMBER

6. AUTHOR(S)
L. Simpson

5d. PROJECT NUMBER
NREL/SR-520-36983

5e. TASK NUMBER
PVB56101

5f. WORK UNIT NUMBER

7. PERFORMING ORGANIZATION NAME(S) AND ADDRESS(ES)
ITN Solar Systems, Inc.
8130 Shaffer Parkway
Littleton, CO 80127-4107

8. PERFORMING ORGANIZATION REPORT NUMBER
ZDO-2-30628-07

9. SPONSORING/MONITORING AGENCY NAME(S) AND ADDRESS(ES)
National Renewable Energy Laboratory
1617 Cole Blvd.
Golden, CO 80401-3393

10. SPONSOR/MONITOR'S ACRONYM(S)
NREL

11. SPONSORING/MONITORING AGENCY REPORT NUMBER
NREL/SR-520-36983

12. DISTRIBUTION AVAILABILITY STATEMENT
National Technical Information Service
U.S. Department of Commerce
5285 Port Royal Road
Springfield, VA 22161

13. SUPPLEMENTARY NOTES
NREL Technical Monitor: R. Mitchell

14. ABSTRACT *(Maximum 200 Words)*

ITN Energy Systems, Inc., and Global Solar Energy, Inc., with the assistance of NREL's PV Manufacturing R&D program, have continued the advancement of CIGS production technology through the development of trajectory-oriented predictive/control models, fault-tolerance control, control-platform development, in-situ sensors, and process improvements. Modeling activities to date include the development of physics-based and empirical models for CIGS and sputter-deposition processing, implementation of model-based control, and application of predictive models to the construction of new evaporation sources and for control. Model-based control is enabled through implementation of reduced or empirical models into a control platform. Reliability improvement activities include implementation of preventive maintenance schedules; detection of failed sensors/equipment and reconfiguration to continue processing; and systematic development of fault prevention and reconfiguration strategies for the full range of CIGS PV production deposition processes. In-situ sensor development activities have resulted in improved control and indicated the potential for enhanced process status monitoring and control of the deposition processes. Substantial process improvements have been made, including significant improvement in CIGS uniformity, thickness control, efficiency, yield, and throughput. In large measure, these gains have been driven by process optimization, which, in turn, have been enabled by control and reliability improvements due to this PV Manufacturing R&D program.

15. SUBJECT TERMS
PV ; module; manufacturer; trajectory-oriented control; fault tolerance; in-situ sensors; sputter deposition; thin-film; real-time composition; small-area; transparent conductive oxide; back contact;

16. SECURITY CLASSIFICATION OF:			17. LIMITATION OF ABSTRACT	18. NUMBER OF PAGES	19a. NAME OF RESPONSIBLE PERSONI
a. REPORT	b. ABSTRACT	c. THIS PAGE			
Unclassified	Unclassified	Unclassified	UL		19b. TELEPONE NUMBER (*Include area code)*

Standard Form 298 (Rev. 8/98)
Prescribed by ANSI Std. Z39.18